TUGAS AKHIR – TM 141585

PEMODELAN DAN ANALISA PENGARUH DAMPER ASIMETRIK TERHADAP KUALITAS KENYAMANAN KENDARAAN

LISTY FAZRIA SETIAWAN
NRP. 2111100180

Pembimbing: Dr. Eng Harus Laksana Guntur ST,M.Eng

PROGRAM SARJANA
LABORATORIUM SISTEM DINAMIS DAN VIBRASI
JURUSAN TEKNIK MESIN
FAKULTAS TEKNOLOGI INDUSTRI
INSTITUT TEKNOLOGI SEPULUH NOPEMBER
SURABAYA
2015

FINAL PROJECT – TM 141585

MODELLING AND ANALYSIS OF THE INFLUENCE OF ASYMMETRICAL DAMPER ON THE RIDE COMFORT OF THE VEHICLE

LISTY FAZRIA SETIAWAN
NRP. 2111100180

Academic Supervisor: Dr. Eng Harus Laksana Guntur ST,M.Eng

DYNAMIC SYSTEM AND VIBRATION LABORATORIUM
DEPARTMENT OF MECHANICAL ENGINEERING
FACULTY OF INDUSTRIAL TECHNOLOGY
SEPULUH NOPEMBER INSTITUTE OF TECHNOLOGY
SURABAYA
2015

APPROVAL SHEET

MODELLING AND ANALYSIS OF THE INFLUENCE OF ASYMMETRICAL DAMPER ON THE RIDE COMFORT OF THE VEHICLE

FINAL PROJECT

Proposed to Fulfill the Requirement to
Obtain the Bachelor Degree
at
Design Study Field
Department of Mechanical Engineering
Faculty of Industrial Technology
Institut Teknologi Sepuluh Nopember

By :
Listy Fazria Setiawan
Nrp. 2111100180

Approved by Board of Examiners :

1. Dr. Eng. Harus Laksana Guntur, ST,M.Eng.....(Supervisor)
   (NIP. 19750511 19990310 01)
2. Dr. Eng. Unggul Wasiwitono, ST, M.Eng. Sc.....(Examiner I)
   (NIP. 19780510 20011210 01)
4. Moch. Solichin, ST., MT.....(Examiner II)
   (NIP.2100201405003)

SURABAYA
January, 2015

PEMODELAN DAN ANALISA PENGARUH DAMPER ASIMETRIK TERHADAP KUALITAS KENYAMANAN KENDARAAN

Nama Mahasiswa	**: Listy Fazria Setiawan**
NRP	**: 2111100180**
Jurusan	**: Teknik Mesin FTI-ITS**
Dosen Pembimbing	**: Dr. Eng Harus Laksana Guntur ST,M.Eng**

Abstrak

Penelitian ini berfokus pada pengaruh karakteristik asimetrik damper pada kualitas kenyamanan penumpang pada mobil yang tipikal. Termotivasi oleh kebutuhan untuk menemukan cara yang efektif namun ekonomis untuk meningkatkan kenyamanan berkendara bagi penumpang, penelitian ini disimulasikan dengan menggunakan data damper asimetrik yang sebenarnya pada mobil penumpang yang tipikal (model mobil seperempat) untuk mengevaluasi kualitas kenyamanannya. Karakteristik damper asimetrik ditunjukkani dengan menggunakan dua konstanta sebagai koefisien redaman, satu ketika suspense sedang kompresi dan satu lagi ketika suspensi perpanjang.

Input transien adalah fungsi dari parameter keparahan, γ yang mewakili keparahan impak, sedangkan input sinusoidal adalah fungsi dari kecepatan kendaraan. Rasio asimetri juga divariasikan untuk mengevaluasi pengaruhnya terhadap tingkat kenyamanan berkendara akibat sistem asimetris.

Dengan berbagai input jalan, variasi parameter keparahan, rasio asimetri serta kecepatan kendaraan, indeks performa dan nilai root-mean-square (RMS) percepatan massa mobil dapat dihitung sehingga efektivitas sistem asimetris dapat

dinilai dengan menggunakan ISO 2631-1 sebagai tolak ukur kualitas kenyamanan penumpang.

Performa kendaraan selama situasi impak berbanding lurus dengan kedua rasio asimetri dan rata-rata, meskipun tidak diketahui oleh berapa banyak masing-masingnya. Namun, perbandingan antara sistem simetris dan asimetris menunjukkan bahwa sistem asimetris, dengan rasio asimetri atas 1, cenderung memiliki performa yang lebih halus dan progresif. Kecenderungan ini meningkat dengan meningkatnya parameter keparahan

Analisis pada input sinusoidal menunjukkan bahwa rasio asimetri tidak memengaruhi peforma kendaraan, hanya rata-rata asimetri saja yang memengaruhi. Pada kecepatan resonansi, model mobil seperempat menunjukkan bahwa semakin tinggi rata asimetri, semakin bagus performa kendaraan. Pada kecepatan lainnya, model mobil seperempat menunjukkan bahwa performa lebih rendah dengan meningkatnya rata-rata asimetri.

<u>Kata kunci</u>: pemodelan, redaman asimetris, respon dinamis kendaraan, sistem suspensi, kenyamanan berkendara

MODELLING AND ANALYSIS OF THE INFLUENCE OF ASYMMETRICAL DAMPER ON THE RIDE COMFORT OF THE VEHICLE

Name : **Listy Fazria Setiawan**
NRP : **2111100180**
Department : **Mechanical Engineering FTI-ITS**
Advisory Lecturer : **Dr. Eng Harus Laksana Guntur ST,M.Eng**

Abstract

This research focuses on the influence of asymmetrical characteristics of dampers on the ride quality of a typical passenger car. Motivated by the necessity to find effective yet economical ways to improve ride comfort for passengers, this research simulated real asymmetrical damper data to a typical passenger car (quarter car model) in order to evaluate its ride quality. The nonlinear asymmetric dampers are conveniently characterized by two constants viscous damping terms, one for compression and another for extension.

Transient inputs are functions of severity parameter, γ that represent severity of impact, while the sinusoidal input is a function of vehicle velocity. The asymmetry ratio is also varied to assess its influence on the apparent improvement in comfort provided by the asymmetrical system.

With different standard road inputs, variation of severity parameter, the asymmetry ratios as well as the velocity of the vehicle, performance indices and root mean square (RMS) values of acceleration of the sprung mass in respect to vehicle velocity are also derived so that the efficacy

of the asymmetrical systems can be assessed using ISO 2631-1 as a measurement of evaluating passenger comfort.

Vehicle performance during impact situations is directly proportional to both asymmetry ratio and average, although it is unknown by how much to each. However, comparison between the symmetrical and asymmetrical systems showed that the asymmetrical system, with asymmetry ratio above 1, tends to have a smoother and more progressive performance. This tendency increases with larger severity of impacts.

Analysis under steady-state input showed that asymmetry ratio does not influence the vehicle performance, only the asymmetry average does. At the resonant velocity, the quarter car model shows that the higher the asymmetry average, the higher is the performance of the vehicle. At any other velocity, the quarter car model shows that the performance is lower the higher the asymmetry average.

Keywords: modelling, asymmetric damping, dynamic responses of vehicle, suspension system, ride comfort

ACKNOWLEDGEMENTS

The author would like to acknowledge the contributions of faculty and students of the Department of Mechanical Engineering at Institut Teknologi Sepuluh Nopember, Surabaya whose help and suggestions have made a positive impact on the completion of the author's final project.

Firstly I would like to use this opportunity to express my deepest gratitude and special thanks to Dr. Eng. Harus Laksana Guntur, ST., M. Eng. as academic advisor who in spite of being busy with his duties, took the time out to hear, guide and keep me on the correct path and allowing me to carry out my final project.

I express my deepest thanks to Prof.Ir. I Nyoman Sutantra, M.Sc.,Ph.D., Dr. Eng. Unggul Wasiwitono, ST, M.Eng. Sc, Dr. Wiwiek Hendrowati, ST., MT., and Moch. Solichin, ST., MT. for taking the roles of the Board of Examiners and giving constructive critics and suggestions. I am most grateful to Ika Dewi Wijayanti, ST.,M.Sc. as Dosen Wali.

I am also deeply indebted to my colleagues Ajeng and Fey at Laboratory of Vibrations and Dynamical Systems as well as the rest of the members of the laboratories in the Design study field for helping me in time of need. A special gratitude I give to the rest of M54 family for always being there and for allowing me to officially convert them M-Gab (by some people's definition, not mine).

I would like to thank my friends from ITS Foreign Language Society (IFLS) as well as members of 'Ibu-Ibu Ceriwis' for taking time to hang out and de-stress together. Finally, I wish to thank my dearest Mama and Papa, sweet Ceuceu and Dede without whose patience, encouragement, and support this final project might never have been completed.

Surabaya, January 2015

Author

This page is left blank intentionally.

TABLE OF CONTENTS

This page is left blank intentionally.

LIST OF TABLES

This page is left blank intentionally.

LIST OF FIGURES

This page is left blank intentionally.

LIST OF NOTATIONS

Z_o = Displacement Due To Road Profile

$\dot{Z}_o$ = Velocity Due To Road Profile

$\ddot{Z}_o$ = Acceleration Due To Road Profile

Z_u = Displacement of Unsprung (Tires)

$\dot{Z}_u$ = Velocity of Unsprung (Tires)

$\ddot{Z}_u$ = Acceleration of Unsprung (Tires)

M_u = Mass of Unsprung (Tires)

K_u = Stiffness of Unsprung (Tires)

C_u = Damping Coefficient of Unsprung (Tires)

Z_s = Displacement of Sprung (Car Body)

$\dot{Z}_o$ = Velocity of Sprung (Car Body)

$\ddot{Z}_o$ = Acceleration of Sprung (Car Body)

M_s = Mass of Sprung (Car Body)

K_s = Stiffness of Sprung (Car Body)

C_s = Damping Coefficient of Suspension

C_s^+ = Damping Coefficient of Suspension When In Extensive Motion

C_s^- = Damping Coefficient of Suspension When In Compressive Motion

γ = Severity Parameter

β = Ratio of Damping Coefficient of Suspension When In Extensive Motion To Damping Coefficient of Suspension When In Compressive Motion

α = Average of Damping Coefficient of Suspension When In Extensive Motion and Damping Coefficient of Suspension When In Compressive Motion

RDR = Relative Displacement Ratio

SDR = Shock Displacement Ratio

SAR = Shock Acceleration Ratio

CHAPTER I
INTRODUCTION

1.1 Research Background

The suspension system on a vehicle has a myriad of purposes. The main objective is to isolate the vehicle from disturbances so that the driver can keep control of the vehicle, without endangering his and the passengers' well-being [1,2]. The disturbances can be caused by irregularities on the road, or caused by loads inherent of the operation of the vehicle, such as acceleration, braking and turning, as well as aerodynamic loads. The loads on the interface between tire and road are of great importance, not only for the vehicle performance, but also for road degradation. Appropriate suspension design may considerably reduce damage inflicted by the vehicle on some types of roads [3]. The cost of the suspension system should also be kept at a minimum in order to improve the commercial attractiveness of the vehicle. Therefore, these many purposes are generally contradictory, making the design of the system a global optimization process.

Classically, a suspension system comprises of symmetrical damping force [4]. However when this damper is exposed to transients which come from impact situations, this configuration does not give the best performance [5]. In normal cars, damping forces are rarely symmetrical [5-7]. To counter that, active and semi-active suspension systems have been proposed [1].

Active and semi-active control of vehicle dynamics itself is always a subject of major interest, and nowadays damping control systems are incorporated in serial constructions of passenger cars. Rapid progress in the analysis, design and technology of the control systems leads to the need for an accurate description of the

dynamics of all components involved, such as the tire or damper [1,6].

It is well-known that automobile dampers are non-linear [5-7], yet so far much modelling is done on assumption that it is linear [8,10]. Although this is good enough for some cases, this linear modelling is of course too poor to describe the power-flow over a broad region of operating conditions [6]. Moreover, some studies have shown that a non-linear damping system can give a smoother and more progressive performance without the added 'cost' of the active or semi-active dampers [2]. Therefore, this research is carried out in order to learn more about the linear asymmetrical damping.

1.2 Problem Formulation

This research is carried out to answer the following questions:

1. How to model and simulate the influence of linear asymmetrical damper on the dynamic responses of the quarter car model.
2. What is the influence of the variations of linear asymmetrical damper angles on the dynamic responses of the quarter car model?
3. Is it possible to conclude the best variations of angles per maximum ride comfort, as standardized by ISO2631? If it is, conclude.

1.3 Research Objectives

The objectives of the research are:

1. To model and simulate the influence of linear asymmetrical damper on the dynamic responses of the quarter car model.
2. To analyse the influence of the variations of linear asymmetrical damper angles on the dynamic responses of the quarter car model.

3. To find out whether it is possible to conclude the best variations of angles for maximum ride comfort, as standardized by ISO2631. If it is, conclude.

1.4 Research Restrictions

This research is carried out keeping in mind with restrictions, such as:

1. The vehicle velocity is constant.
2. The quarter car model is a 2DOF system.
3. The vehicle is assumed to be moving in a straight line.
4. The parameters used when simulating the quarter car model are taken from a typical passenger car.

1.5 Research Benefits

This research is carried out for benefits such as:

1. To provide recommendation on the asymmetrical damper angle for the best ride comfort.
2. To give comparison on how asymmetrical damper influence dynamic responses, as compared to symmetrical damper.

This page is left blank intentionally.

CHAPTER II
LITERATURE STUDIES

2.1 Literature Studies

The automotive suspension on a vehicle has always been a subject of major interest. Not only it has to be able to support the vehicle static weight and to isolate a car body from road disturbances, it has to enable good road holding as well as good handling. Apart from these basic operational aspects, the suspension should provide a good level of comfort for the passengers, minimizing the movements and accelerations imposed on and perceived by them [1,2]. Although the most common suspension system is still passive suspension, it is well known that they are not ideally suited to the whole range of operational conditions and purposes. Analysis of passive suspensions in a quarter car model shows that there are significant trade-offs in performance between the ride quality, road holding and its ability to support the vehicle static weight [1]. In order to get improved performance in all these aspects, researchers have suggested various kinds of suspension.

Active suspensions and semi-active suspensions are now often used as they give superior performance than passive suspensions. Active suspension is a system with compressors, hydraulic pumps and actuators that requires an input of energy, while semi-active suspension consists of a twin tube viscous damper in which the damping coefficient can be varied by changing the diameter of orifice [1]. Despite having very good efficacy (more so the active suspension), the considerable increase in complexity, involving sensors, actuators, considerations of power consumption and thus the extra cost that comes with it can actually lower the commercial attractiveness of the vehicle. Although the level of comfort is increasingly seen as one of the main contributing factors for purchase decision, the

cost of this comfort level still has to be kept at a minimum so that the vehicle can remain competitive in market [2]. Such contradictory criteria therefore require the design of the suspension to be an optimization.

The classic theory of mechanical vibrations usually considers a viscous damper which acts as a continuous and proportional way to the required velocity, i.e. it acts in a linear and symmetrical manner [4, 8,10]. However when this damper is exposed to transients which come from impact situations, this configuration does not give the best performance [5]. Several studies have proposed a solution of adopting a viscous damper that acts in an asymmetrical way, i.e. it has larger dissipation effect in the opposite direction of the usual impact situation [2,6,11,12]. Moreover, there are experimental data that show that automotive dampers are indeed non-linear dynamical systems as in Figure 2.1[6,7].

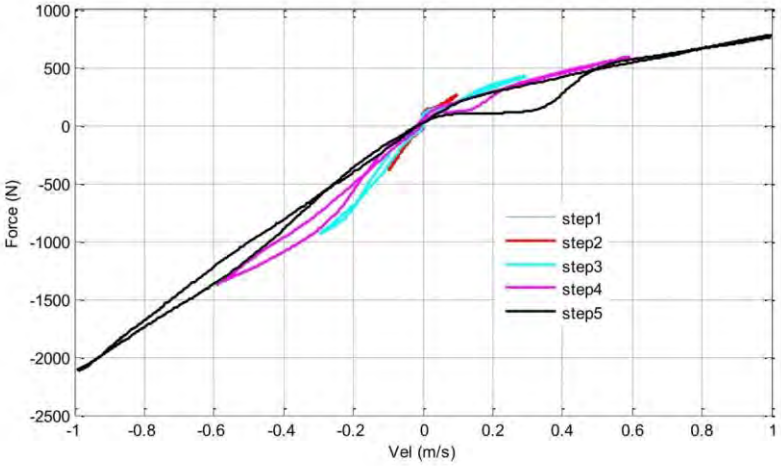

Fig. 2.1 A Damping Force- Velocity Diagram Acquired From Dampers of an Angguna Car [7]

Wallaschek [6] discussed the methods of harmonic and stochastic linearization in respect to applications in damper dynamics. With the use of experimental data, he argued that various simple physical interpretations of the experimental results can be obtained for a typical passenger car's shock-absorber. Wallaschek applied harmonic motion with frequency of 1 Hz to the damper to produce the force-displacement and force-velocity diagrams as in Figure 2.2. He then analysed the effects of asymmetry by using the discussed methods.

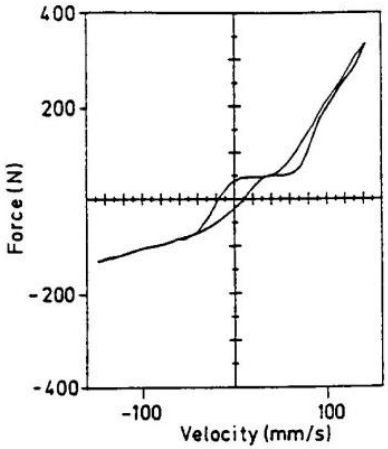

Fig. 2.2 Force-Velocity Diagram [6]

Wallaschek's data showed that dampers behave asymmetrically. He wrote that the force-velocity characteristic of the damper can be described by two constants viscous damping terms, one for compression and another for extension. Wallaschek however concluded that the best way to describe the dynamics of a damper – at least for harmonic or stationary random motion – seems to be the direct use of an equivalent linear model whose

parameters are estimated using the experimental techniques he described.

Ahmed et al in 1992 [11] had used the same equivalent linearization technique as Wallaschek but took it further by analyzing the asymmetric dampers' ride quality. Since the ride quality analyses are primarily performed in the frequency domain, the nonlinear asymmetric dampers are conveniently characterized by either linear or linear equivalent force-velocity characteristics. They adopted a model employing dampers with multi-phase and asymmetric characteristics in compression and extension to achieve improved ride quality or handling trade-off. The dampers are designed to yield high damping corresponding to low velocity, to achieve improved control of handling, and yield low damping at high velocity to improve vibration isolation and ride quality as in Figure 2.3.

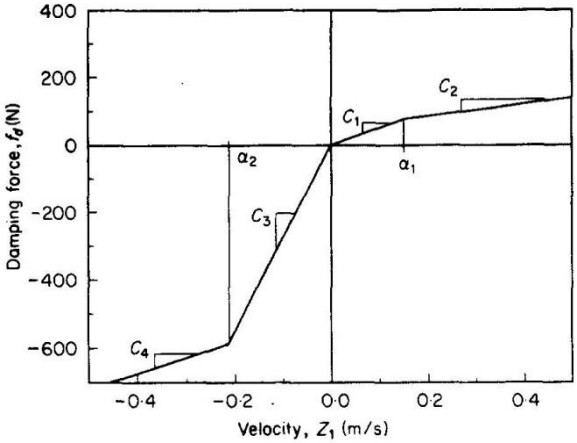

Fig. 2.3 Typical Force-Velocity Characteristics of a Hydraulic Damper [11]

In 1994, Ahmed et al [12] had again proposed a different linearization technique to analyze asymmetric dampers. Frequency response characteristics of mechanical

systems with symmetric and asymmetric restoring and dissipative components are evaluated using a local equivalent algorithm based upon principle of energy similarity. The equivalent models, formulated as a function of local excitation frequency and amplitude, are solved in the convenient frequency domain and the response characteristics are compared with those derived from integration of nonlinear differential equations. A comparison of the results revealed that the magnitude of response error for symmetric elements is higher than that of asymmetric elements, yet it can be considerably reduced using the force similarity.

Rajalingham et al [14] in 2003 had analyzed the influence of suspension damper asymmetry on the vehicle vibration response due to ground excitation using the quarter car model. They assumed that the non-linear suspension damper to have different damping coefficients for compressive and expansive motions of the suspension, much like many suggested before. The study however was done to enhance an understanding of the mechanism associated with the downward shifting of the sprung mass.

Motivated by the necessity to find effective yet economical ways to improve ride comfort for passengers, Silveira et al [2] compared the behaviour of two different types of dampers - symmetrical (linear) and asymmetrical (non-linear) – for use on passenger vehicles. In their study, Silveira et al utilised simplified parameters of asymmetrical damper suggested by Wallaschek which is to assigned two constants viscous damping terms, one for compression and another for expansion. The following force-velocity diagram in Figure 2.4 and mathematical function (2.1) of the quarter-car model Silveira et al used illustrated the simplified parameters.

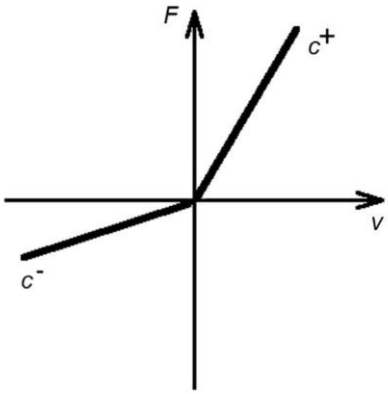

Fig. 2.4 Generic Asymmetrical Characteristic of a Damper [2]

$$D(\dot{z_s} - \dot{z_u}) = \begin{cases} c_s^+ \; if \; \dot{z_s} - \dot{z_u} \geq 0 \\ c_s^- if \; \dot{z_s} - \dot{z_u} < 0 \end{cases} \text{.....(2.1)}$$

Silveira et al utilised standard road inputs as functions of severity parameter, γ. The effect of γ can be seen in these figure, as it assumes the values 1 (low impact), 5 (less severe impact) and 20 (more severe impact). Larger values of γ may represent an irregularity which is hit at a higher velocity, or a sharper irregularity which the latter case can be seen in Figure 2.5. The asymmetry ratio ($\beta = \frac{c^+}{c^-}$) was then varied by Silveira et al to assess its influence on the apparent improvement in comfort provided by the asymmetrical system.

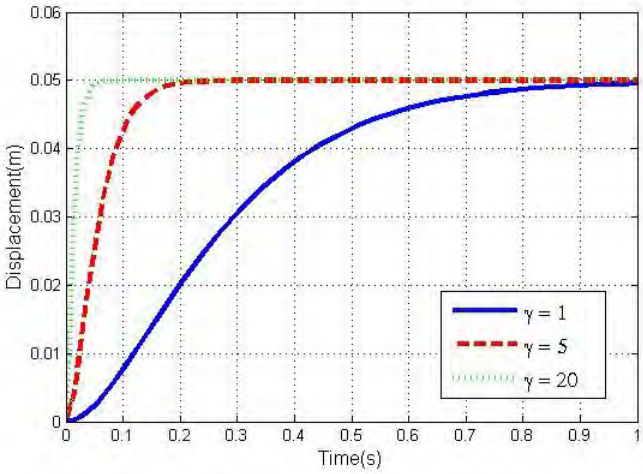

Fig. 2.5 Modified Step as Road Input With Different Severity Parameters

With different standard road inputs, variation of severity parameter, the asymmetry ratios as well as the velocity of the vehicle, performance indices and acceleration values are derived so that the efficacy of the asymmetrical systems can be assessed. The performance indices include relative displacement ratio (RDR), shock displacement ratio (SDR) and shock acceleration ratio (SAR). Their respective equations are given below: [2]

$$RDR = \left|\frac{(z_s - z_o)}{z_{o,max}}\right|_{max},\ SDR = \frac{|z_{s,max}|}{z_{o,max}},\ SAR = \frac{|\ddot{z}_{s,max}|}{|\ddot{z}_{o,max}|} \quad \ldots\ldots(2.2)$$

Their study showed that the asymmetrical system tends to have a smoother and more progressive performance, both for vertical and angular movements. During the simulation of the half-car model, Silveira et al found that the use of asymmetrical system only at the front of the vehicle can further diminish the angular oscillations.

Ultimately they recommended the use of asymmetrical systems for vibrations and impact absorption.

Passenger comfort is a key issue in design and manufacture of modern automobiles. The level of comfort of passengers depends on the amplitude and frequency of vibrations, as well as on direction. One of the most common methods used for measurements of vibrations affecting humans are the ones described in the ISO 2631-1 [13]. As per this standard, passenger comfort principally depends on the root mean square (RMS) value of acceleration and the frequency of vibrations on his body.

Since a particular vibration condition may be considered to cause unacceptable discomfort in one situation but may be classified as pleasant or exciting in another, many factors combined to determine the degree to which discomfort may be noted or tolerated. Comfort expectations and annoyance tolerance are quite different in transportation vehicles compared to commercial or residential buildings. Moreover, interference with activities, i.e. reading, writing, drinking, due to vibration may sometimes be considered a cause of discomfort.

Studies have shown the following values in Table 2.1 give approximate indicators of likely reactions to various magnitudes of overall vibration total values in public transport. However the reactions at various magnitudes depend on passenger expectations with regard to trip duration and the type of activities they are engaging in. Figure 2.6 also shows the values of accelerations accepted to allow comfort.

Table 2.1 Acceptable Value of Vibration Magnitude For Comfort [13]

Magnitude	Comfort Levels
$a < 0.315\ m/s^2$	Not uncomfortable
$0.315\ m/s^2 < a < 0.63\ m/s^2$	A little uncomfortable
$0.5\ m/s^2 < a < 1\ m/s^2$	Fairly uncomfortable
$0.8\ m/s^2 < a < 1.6\ m/s^2$	Uncomfortable
$1.25\ m/s^2 < a < 2.5\ m/s^2$	Very uncomfortable
$a > 2\ m/s^2$	Extremely uncomfortable

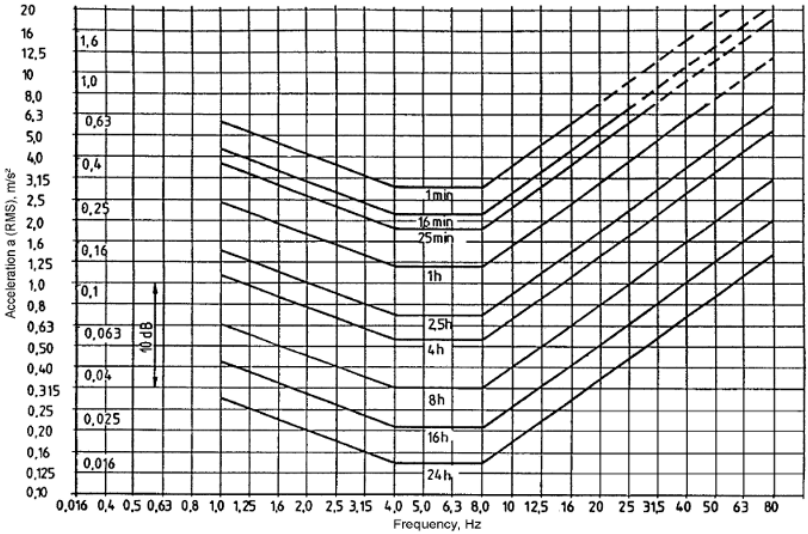

Fig. 2.6 Graph of Exhaustion Limit Due To Receiving Vertical Vibrations [13]

2.2 Basic Concepts

2.2.1 The Theory of Vibration

1. Definition of Vibration

Any motion that repeats itself after an interval of time is called vibration or oscillation [4]. For instance, typical examples of vibration are the swinging of a pendulum or the motion of a plucked string on a guitar. A vibratory system, in general, includes a means of storing potential energy (spring or elasticity), a means for storing kinetic energy (mass or inertia), and a means by which energy is gradually lost (damper) [4]. Therefore, the vibration of a vibratory system involves the transfer of its potential energy and of its kinetic energy to potential energy, alternately. This is demonstrated nicely in the swinging of a pendulum.

Mass or inertia, spring or elasticity and damper are elementary parts of a vibratory system. Figure 2.7 is an illustration of the elementary parts along with their symbols.

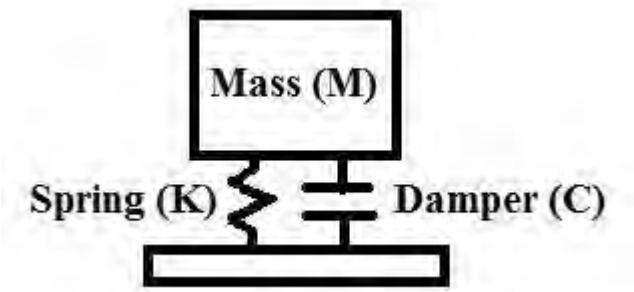

Fig. 2.7 A 1DOF Mass-Spring-Damper System

2. Degree-of-freedoms (DOF)

The minimum number of independent coordinates required to determine completely the positions of all parts of a system at any instant of time defines the number of degree-of-freedoms (DOF) of the system. [4]

3. Equation of Motion

Equations of motion are the governing equations derived from each mass or inertial body and its interaction with other elements of the vibratory system in order to study the response of the system. In order to derive the equations of motion, one must first study the equations governing how energy is stored or dissipated in the elements of a vibratory system.[4]

Potential Energy (V) of equivalent spring coefficient (k_{eq} or $k_{t,eq}$):

$$V = \sum_{i=1}^{\infty} \frac{1}{2} k_i x_i^2 + \sum_{j=1}^{\infty} \frac{1}{2} k_j \theta_j^2 = \frac{1}{2} k_{eq} {x_{eq}}^2 \quad \text{.....(2.3)}$$

Kinetic Energy (T) of equivalent mass (m_{eq}) or inertia (J_{eq}):

$$T = \frac{1}{2} m \dot{x}^2 + \frac{1}{2} J \dot{\theta}^2 = \frac{1}{2} k_{eq} {\dot{x}_{eq}}^2 \text{ or } \frac{1}{2} k_{t,eq} \dot{\theta}^2 \quad \text{.....(2.4)}$$

Damping Energy (D) of equivalent damping coefficient (c_{eq}):

$$D = \sum_{i=1}^{\infty} \frac{1}{2} c_i \dot{x}_i^2 = \frac{1}{2} c_{eq} \dot{x}^2 \quad \text{.....(2.5)}$$

With knowledge of these equations governing the elementary parts of a vibratory system, one can find the equations of motion of a vibratory system using either one the following methods:

Newton's Second Law of Motion

$$\sum F = m\ddot{x} \text{ and } \sum M = I\,\ddot{\theta} \quad \text{.....(2.6)}$$

Energy Method

$$\frac{d}{dt}[T + V] = 0 \quad \text{.....(2.7)}$$

Lagrange Method

$$\frac{d}{dt}\left[\frac{\partial L}{\partial \dot{x}}\right] - \frac{\partial L}{\partial x} + \frac{\partial D}{\partial \dot{x}} = 0 \quad \text{.....(2.8)}$$

Where: $L = T - V$

$D = \frac{1}{2}c\dot{x}^2$

4. Response of a Vibratory System

The solution to a vibratory system consists of equations in terms of time that represent the motion of the vibratory system. This is usually known as the response of a vibratory system. [4]

The response of a vibratory system varies greatly with the excitation that causes the system to vibrate, i.e. free vibration, harmonic vibration, periodic vibration, non-periodic vibration, base excitation, etc. However, the procedure to find the solution of a vibratory system is still fairly simple whatever kind of excitation causes the vibration. First by deriving the equation of motion of the system, then by using assumptions of displacement –

assumptions vary with the kind of excitation – one can derive the response of a vibratory system.

In the case of free vibration as the excitation, the vibratory system will give a response known as a transient or homogeneous response. Under harmonic vibration though, the response of the vibratory system can be categorized into two: transient response and steady or particular response. The transient response will die out after the initial excitation, while the steady response will be present as long as the forcing function is present.

Transient or Homogeneous Response

The transient response comes about to suddenly applied non-periodic excitation, i.e. a bump on the road. With time, the response will die out to let the system stabilize.

The equation of motion in order to find the solution to the transient part of the system response is:

$m\ddot{x} + c\dot{x} + kx = 0$……..…….(2.9)

Steady or Particular Response

The steady response of the vibratory system refers to the response the system produces under the influence of a forcing function while it is applied. Below is the illustration of a steady response.

The equation of motion in order to find the solution to the steady part of the system response in which F(t) is the forcing function present during harmonic vibration excitation is:

$m\ddot{x} + c\dot{x} + kx = F(t)$……..……..(2.10)

5. Response of a Damped System Under the Harmonic Motion of the Base

A common case in which a system of mass, spring and damper is harmonically excited can be observed in Figure 2.8.

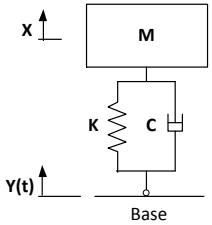

Fig. 2.8 A Mass-Spring-Damper System

Excitation y(t) represents base displacement, while x(t) represents the displacement of mass relative to its steady-state position. Both y(t) and x(t) are functions of time. Figure 2.9 shows the free body diagram of the case above.

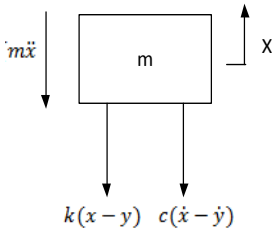

Fig. 2.9 Free Body Diagram of System Described in Fig. 2.8

rom the free body diagram above, an equation of motion can be derived. (-y) represents elongation of spring, while (-y) the relative velocity of the damper.

$$m\ddot{x} + c(\dot{x} - \dot{y}) + k(x - y) = 0 \text{……..…(2.11)}$$

Assuming $y(t) = Y \sin \omega t$, the equation becomes:

$$\begin{aligned} m\ddot{x} + c\dot{x} + kx &= ky + c\dot{y} \\ &= kY \sin \omega t + c\omega Y \cos \omega t \\ &= A \sin(\omega t - \alpha) \text{……..…(2.12)} \end{aligned}$$

Where: $A = Y\sqrt{k^2 + (c\omega)^2}$

$$\alpha = \tan^{-1}\left[-\frac{c\omega}{k}\right]$$

This shows that base excitation is equivalent to a harmonic force of value A to the mass. The steady-state response can be represented as:

$$x_p(t) = \frac{Y\sqrt{k^2+(c\omega)^2}}{[(k-m\omega^2)^2+(c\omega)^2]^{1/2}} \sin(\omega t - \phi_1 - \alpha) \text{...(2.13)}$$

Where: $\phi_1 = \tan^{-1}\left[\frac{c\omega}{k-m\omega^2}\right]$

Using trigonometry, the equation can be simplified to:

$$x_p(t) = X \sin(\omega t - \phi) \text{…..(2.14)}$$

In which:

$$\frac{X}{Y} = \left[\frac{k^2+(c\omega)^2}{(k-m\omega^2)^2+(c\omega)^2}\right]^{1/2} = \left[\frac{1+(2\zeta r)^2}{(1-r^2)^2+(4\zeta^2-1)r^2}\right]^{1/2} \text{……...(2.15)}$$

$$\phi = \tan^{-1}\left[\frac{mc\omega^3}{k(k-m\omega^2)+(c\omega)^2}\right] = \tan^{-1}\left[\frac{2\zeta r^3}{1+(c\omega)^2}\right] \text{……...(2.16)}$$

The displacement transmissibility

The ratio of the amplitude of the response $x_p(t)$ to that of the base motion, $y(t)$, $\frac{X}{Y}$, is called the displacement transmissibility as in Figure 2.10[4].

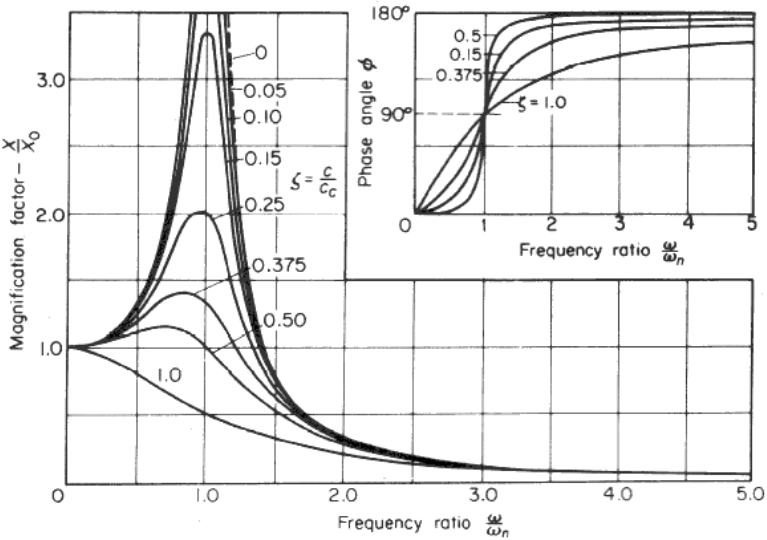

Fig. 2.10 A Transmissibility Displacement – Frequency Ratio Graph

The following aspects of displacement transmissibility, $T_d = \frac{X}{Y}$, can be noted from:

1. The value of T_d is unity at r = 0 and close to unity for small values of r.
2. For an undamped system (ζ=0), T_d → ∞ at resonance (r = 1).
3. The value of T_d is less than unity (T_d < 1)for values of ζ at $r > \sqrt{2}$ (for any amount of damping ζ).
4. The value of T_d is unity for all values of ζ at $r = \sqrt{2}$.

5. For $r < \sqrt{2}$, smaller damping ratios lead to larger values of T_d. On the other hand, for $r > \sqrt{2}$, smaller values of damping ratios lead to smaller values of T_d.
6. The displacement transmissibility, T_d, attains a maximum for $0 < \zeta < 1$ at the frequency ratio $r = r_m < 1$ given by:

$$r_m = \frac{1}{2\zeta}\left[\sqrt{1+8\zeta^2}-1\right]^{1/2} \quad \text{.....(2.17)}$$

6. Multi degree-of-freedom (DOF) Systems

A multi degree-of-freedom (DOF) system requires more than one number of independent coordinates to determine completely the positions of all parts of a system at any instant of time [4]. Below in Figure 2.11 is a 2-DOF system below.

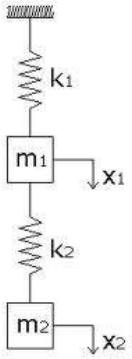

Fig. 2.11 A 2-DOF System

The procedure of analysing the system above can be summarized into steps below:

1. Set up suitable coordinates to describe the positions of the masses and rigid bodies in the system. Assume suitable positive directions for the displacements,

velocities and accelerations of the masses and the rigid bodies.

2. Determine the static equilibrium configuration of the system.
3. Draw the free body diagram of each mass and rigid body in the system.
4. Apply Newton's second law of motion to each mass and rigid body shown by the free body diagrams as:
   $m_i\ddot{x}_i = \sum_j F_{ij}$ (for mass *i)*
   Or
   $J_i\ddot{\theta}_i = \sum_j M_{ij}$ (for rigid body of inertia i)
5. Using Lagrange, equation of motion can be derived. Lagrange equation for *n* degree-of-freedom is as followed:

$$\frac{d}{dt}\left(\frac{\partial T}{\partial \dot{q}_j}\right) - \frac{\partial T}{\partial q_j} + \frac{\partial V}{\partial q_j} = Q_j^{(n)} \quad , j = 1, 2, ..., n \ldots..(2.18)$$

   In which $\dot{q}_j = \partial q_j/\partial t$ is velocity and $Q_j^{(n)}$ is non-conservative force. When only conservative forece presents, $Q_j^{(n)} = 0$.
6. Besides, using Lagrange equation, equation of motion can be solved using software Simulink Matlab. This will be explained in later chapter.

2.2.2 System Modelling

1. State-Variable Modelling

State-variable modelling requires the equation motion to be converted into another form as shown below. By assuming the following: $\dot{x} = v$ and $\ddot{x} = \dot{v}$, the equation of motion is then converted [9]:

$$m\ddot{x} + c\dot{x} + kx = F(t) \qquad \rightarrow \qquad m\dot{v} + cv + kx = F(t)$$

$$\dot{v} = \frac{1}{m}\left[F(t) - cv - kx\right] \text{ ……..(2.19)}$$

A general representation of state variable equations in matrix form is shown below.

$$\{\dot{q}\} = [A]\{q\} + [B]\{u\} \text{ ……...…(2.20)}$$

2. Simulink MATLAB

To see the response of a vibratory system, the software Simulink Matlab can be utilised as per in this final project. Simulink itself is a software extension of Matlab that allows users to simulate modelling of a dynamic system on a computer accurately using block diagram notation from its library browser.

Simulink can be used simultaneously with Matlab. For example, after creating the Simulink model file and m-file, one can simply summon the Simulink model by writing a certain command on the m-file.

This page is left blank intentionally.

CHAPTER III
RESEARCH METHODOLOGY

In this paper, the influence of asymmetrical damping force on dynamic responses of quarter car model is studied. The study is carried out according the following processes as in Figure 3.1:

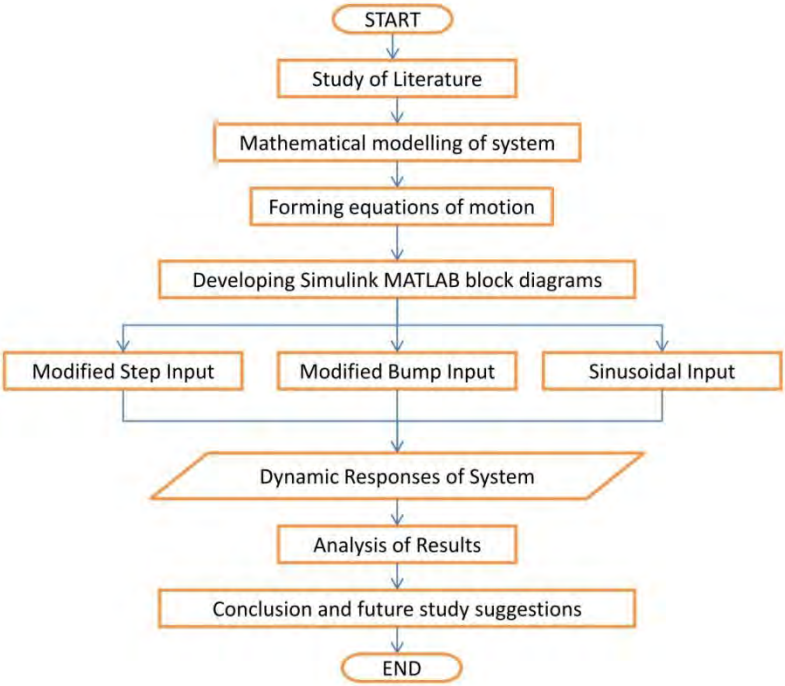

Fig. 3.1 Flowchart of the Influence of Asymmetrical Damping Force on The Dynamic Responses of Quarter Car Model

This research is generally carried out according to the flowchart in Fig.3.1. First, a study of literature is done concerning the asymmetrical characteristics of dampers and factors concerning ride comfort for a typical passenger car. The parameters of the chosen passenger car are collected, and

modelling is done using the well-known quarter car model. Equations of motion are used in the form of state variable equations to build block diagrams in Simulink MATLAB. Outputs such as time responses, performance indices and RMS accelerations in the frequency form of responses are analyzed and conclusions are then drawn.

3.1 During Study of Literature

In this paper, prior studies are needed to support the analysis of the influences of asymmetrical damping force on dynamic responses of quarter car model. Therefore, study of literature is done to support and serve as foundation of this study. Supporting data of system modelling can be found in books. Other than that, scientific journals are used to serve as additional references.

3.2 During Mathematical Modelling of System

In this paper, one type of model is being observed - a quarter car model. This model is derived from an automotive vehicle as in Figure 3.2. Inputs that are used are road excitation in forms of both transient (modified step and bump) and steady state (sinusoidal). The dynamic responses are used in determining the ride comfort level according to ride comfort standard ISO 2631-1.

Fig. 3.2 A Typical Passenger Sedan Car

Figure 3.3 is a mathematical model of a quarter car with 2 degrees of freedom (DOF). Modelling includes Ms (sprung mass) which represents the car body mass and Mu

(unsprung mass) which represents the tires mass. Ks and Ku represent the suspension and the tires stiffness, respectively. Correspondingly, Cs and Cu represent the suspension and the tires damping coefficients.

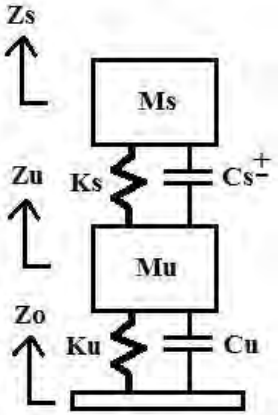

Fig. 3.3 A Quarter Car Model

3.3 During Forming Equations of Motion

The process of forming equations of motion of the quarter car model can be represented on the flowchart following in Figure 3.4:

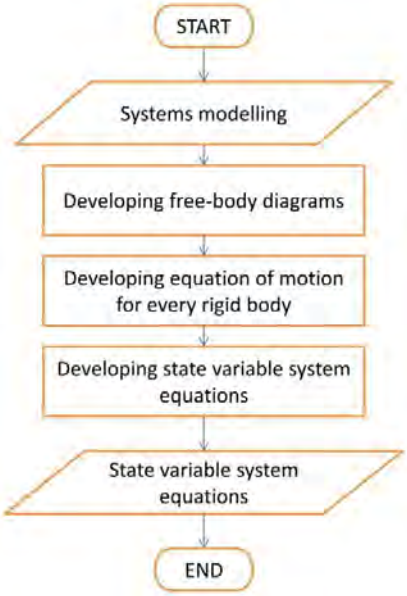

Fig. 3.4 Flowchart of the Process of Forming Equations of Motion

3.4 Developing Simulink MATLAB Block Diagrams

Equations of motion in the form of state variable are then used to build block diagrams in Simulink MATLAB. Block diagrams are developed using the software Simulink Matlab in order to be able to generate the desirable outputs. Executions of programme are done using three kinds of input: modified step input, modified bump input and the sinusoidal input. The modified step and bump inputs are functions of severity parameter, γ. The effect of γ in both inputs can be seen, as it assumes the values 1 (low impact), 5 (less severe impact) and 20 (more severe impact). Larger values of γ may represent an irregularity which is hit at a higher velocity, or a sharper irregularity. The sinusoidal input is a function of the vehicle velocity. Three variations are utilised, as it presumes the values of 40 km/hr (low

speed), 60 km/hr (medium speed) and 80 km/hr (high speed).

Variations of damping coefficient for compressive and expansive motion of the suspension, c_s^- and c_s^+, are used in addition to the original experimental data of the asymmetrical damper of the Angguna car as can be seen in Table 3.1. The influences of asymmetry ratio $\beta = \frac{c^+}{c^-}$ and asymmetry average $\alpha = \frac{c^+ + c^-}{2}$ are assessed, too. The responses produced are time responses as well as the frequency responses corresponding to different velocities.

Table 3.1 Variations of Damping Coefficients for Compressive and Expansive Motion of the Suspension

			Csplus (Ns/m)		
			350	2000	4000
Csmin (Ns/m)	1430	β	0.24476	1.3986	2.7972
		α	890	1715	2715
	2000	β	0.175	1	2
		α	1175	2000	3000
	4000	β	0.0875	0.5	1
		α	2175	3000	4000

The process of developing the block diagrams is summarized on the flowchart in Figure 3.5.

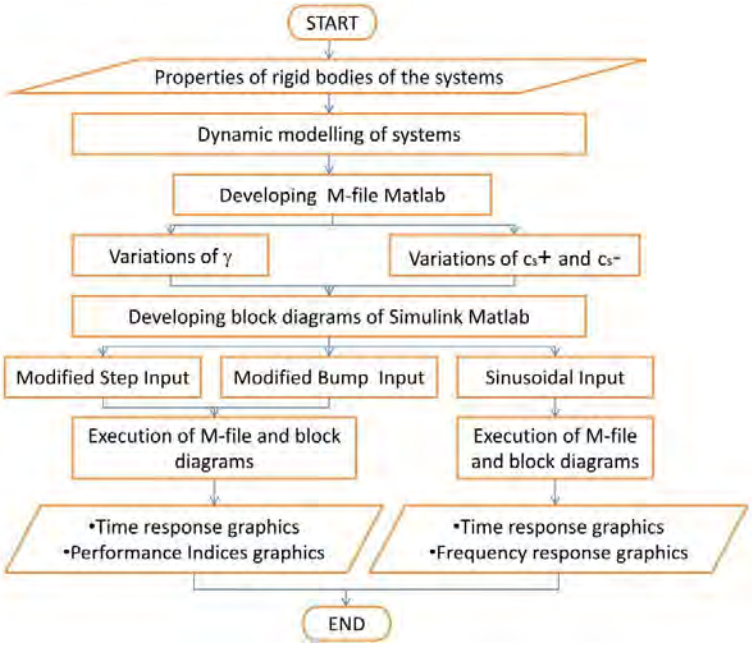

Fig. 3.5 Flowchart of Developing Block Diagrams in Simulink MATLAB

3.5 During Analysis of Results

By modelling using Simulink MATLAB, dynamic responses output including the displacement, velocity and acceleration graphics with different inputs (modified step, modified bump and sinusoidal inputs) as functions of severity parameter or vehicle velocity. Graphics produced include time responses graphics and performance indices as well as RMS acceleration in the form of the frequency responses. Effects of variations of damping coefficient of the suspension can be seen through these graphics. Graphics will be then analysed and evaluated according to the ISO 2631-1 standard for ride comfort.

Conclusions that are drawn will cover several points. First, a conclusion with regards of the time responses of the quarter car modelling due to different inputs i.e. modified

step and bump input, and the sinusoidal input. Second, a conclusion that concerns the difference of symmetrical damping and asymmetrical damping on the effects of the time responses of the quarter car modelling with different inputs. Third, conclusions with reference to the level of ride comfort produce with different combinations of the variations of the damping coefficients. For the transient inputs, performance indices are used to measure level of comfort while for steady state input, RMS acceleration in the form of frequency response are used with reference to the ISO 2631-1.

This page is left blank intentionally.

CHAPTER IV
SYSTEM MODELLING

4.1 Mathematical Modelling of System

The model that is used in this final project is a quarter car model with 2 degree-of freedom, as illustrated below in Fig. 4.1.

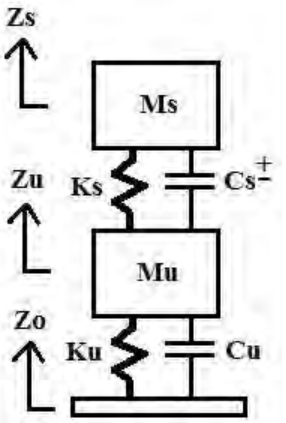

Fig. 4.1 A Quarter Car Model with Two Damping Coefficients c_s^+ and c_s^-

From the figure above, a system of 2 degree-of-freedom consists of the unsprung mass (Mu) which represents the tires that moves in the direction of Zu and the sprung mass (Ms) which represents the body of the car that moves in the direction of Zs. Zo represents the road profile that will become the input for the quarter car model. According to the quarter car model illustrated above, the following free body diagrams (FBDs) can be generated.

1. FBD of the unsprung mass

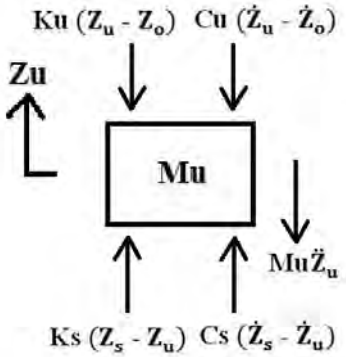

Fig. 4.2 Free-Body-Diagram of the Unsprung Mass

The equation of motion that can be derived from the FBD above in Figure 4.2 is shown below.

$$M_u\ddot{Z}_u - C_s(\dot{Z}_s - \dot{Z}_u) - K_s(Z_s - Z_u) + C_u(\dot{Z}_u - \dot{Z}_o) + K_u(Z_u - Z_o) = 0 \quad \text{.....(4.1)}$$

The equations of motion above can be used to develop state variable system equations. The equation of motion of the unsprung mass can be converted into the following state variable system equation.

$$\dot{Z}_u = v_u \quad \text{.....(4.2)}$$

$$\dot{v}_u = \frac{1}{M_u}(C_s(\dot{Z}_s - \dot{Z}_u) + K_s(Z_s - Z_u) - C_u(\dot{Z}_u - \dot{Z}_o) - K_u(Z_u - Z_o)) \quad \text{.....(4.3)}$$

2. FBD of the sprung mass

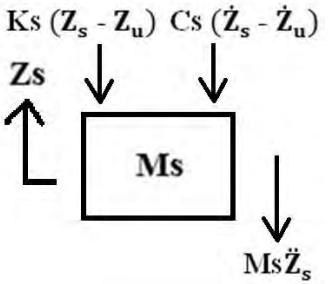

Fig. 4.3 Free-Body-Diagram of the Sprung Mass

The equation of motion that can be derived from the FBD in Figure 4.3 is shown below.

$$M_s\ddot{Z}_s + C_s(\dot{Z}_s - \dot{Z}_u) + K_s(Z_s - Z_u) = 0 \quad \text{.....(4.4)}$$

The equations of motion above can be used to develop state variable system equations. The equation of motion of the sprung mass can be converted into the following state variable system equation.

$$\dot{Z}_s = v_s \quad \text{.....(4.5)}$$

$$\dot{v}_s = \frac{1}{M_s}(-C_s(\dot{Z}_s - \dot{Z}_u) - K_s(Z_s - Z_u)) \quad \text{.....(4.6)}$$

4.2 Modelling Using Simulink MATLAB

4.2.1 Modelling of System

State variable system equations are then used to develop the system block diagrams in Simulink MATLAB

as shown in Figure 4.4. Road excitations act as inputs to this quarter car system and the outputs are sent to workspace at the end of simulation. The outputs are displacements of unsprung mass, sprung mass and road, velocities of unsprung mass, sprung mass and road, accelerations of unsprung mass, sprung mass and road as well as the root-mean-square acceleration of sprung mass.

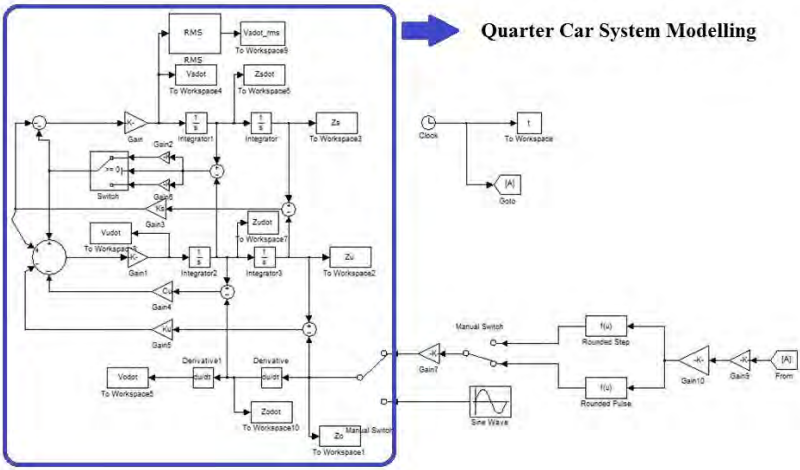

Fig. 4.4 Quarter Car System Modelling Using Simulink

4.2.2 Input Modelling

For simulation using MATLAB, first different inputs must be determined. The irregularities of the road on which the vehicle travels are modelled according to the characteristics intended to be analysed. It is possible to choose an appropriate model from sinusoidal, impulse and step among others.

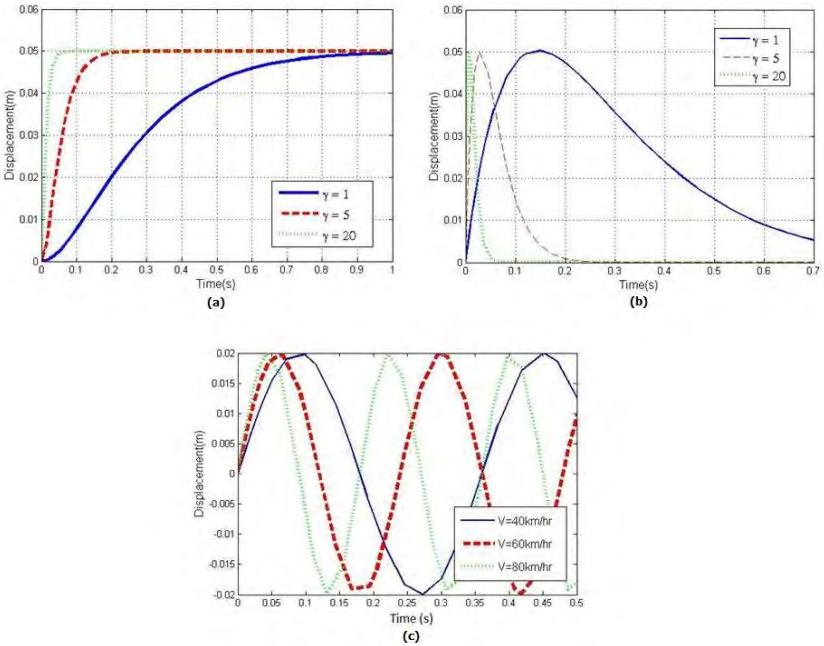

Fig. 4.5 Modified step (a), bump (b) and sinusoidal (c) profiles with severity parameter γ or vehicle velocities

Along with a sinusoidal model to assess steady-state response of the vehicle suspension, shown in Figure 4.5 (c), two road displacements are used for vehicle suspension analysis concerning shock loads are the modified step and bump, shown in Figure 4.5 (a) and (b), and defined by their respective functional forms in the equations below. The standard inputs are used to represent a discrete irregularity on the road, such as a bump or a vertical mismatch between sections of the pavement.

$$Z_o(t) = Z_{max}(1-(1+\gamma\omega_o t)e^{-\gamma\omega_o t}) \quad \text{.....(4.7)}$$

$$Z_o(t) = Z_{max}0.37e^2(\gamma\omega_o t)e^{-\gamma\omega_o t} \quad \text{.....(4.8)}$$

$$Z_o(t) = Amp \cdot \sin(\omega t) \quad \text{.....(4.9)}$$

Equation 4.7 is of the modified step input, while equation 4.8 is of the modified bump input. In these equations, Z_{max} is the maximum amplitude of the road amplitude, γ is the severity parameter, ω_o is defined as $\sqrt{k_s/m_s}$ and t is the time. The effect of γ can be seen in these figures, as it assumes the values 1 (low impact), 5 (less severe impact) and 20 (more severe impact). Larger values of γ may represent an irregularity which is hit at a higher velocity, or a sharper irregularity. In this work, we consider the latter. The maximum amplitude of the road input (Z_{max}) was set to 5cm, representative of standards to assess comfort for vehicles.

In equation 4.9, the sinusoidal input has amplitude, Amp of 2 cm, ω is defined as $2\pi v/\lambda$, and wavelength λ of 4 m. For the sinusoidal input, three types of speed are used: 40 km/hr for low speed, 60 km/hr for medium speed and 80 km/hr for high speed.

These equations are used in developing Simulink block diagrams for the modelling of the road excitation inputs, shown in Figure 4.6. Running simulation requires choosing manually one road excitation input and running an M-file.

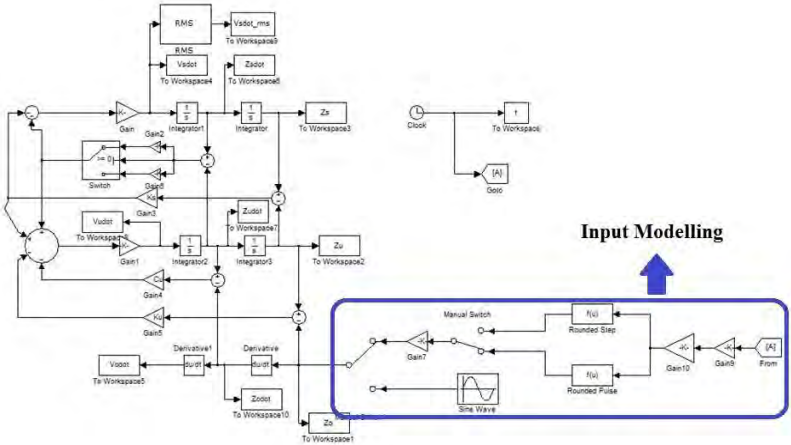

Fig. 4.6 Input Modelling Using Simulink

4.3 Output Generation Using MATLAB

4.3.1 Time Responses

After determining the different road excitation inputs and modelling them using Simulink block diagrams, time responses outputs can be generated using the system model along with the manually chosen road excitation input.

These time responses outputs are generated on command from the M-files developed for both the transient inputs i.e. modified step and bump inputs and the sinusoidal input. Variations of the severity parameter – in transient cases - or vehicle velocity –in sinusoidal case- as well as variations of suspension damping coefficients are included in the M-file.

4.3.2 Ride Comfort Evaluation

Performance indices for transient cases or root-mean-square accelerations of sprung mass – for sinusoidal cases- are generated to evaluate the level of comfort

provided by the different combinations of the variations of the suspension damping coefficients.

These outputs are generated on command from the M-files developed for both the transient inputs i.e. modified step and bump inputs and the sinusoidal input. Variations of the severity parameter – in transient cases - or vehicle velocity –in sinusoidal case- as well as variations of suspension damping coefficients are included in the M-file. For ride comfort evaluation, first scatter graphs are generated using MATLAB and then the data is collected and used to generate various graphs via the software Minitab to get a better representation of the ride comfort of the vehicle in respect to different factors i.e. severity parameter (γ), asymmetry ratio (β) and asymmetry average (α).

4.4 Modelling Variables and Parameters

4.4.1 Modelling Variables

Variations of damping coefficient for compressive and expansive motion of the suspension, c_s^- and c_s^+, are used in addition to the original experimental data of the asymmetrical damper of the Angguna car. These damping coefficients are combined to produce 9 combinations as shown in Figure 4.7. Combination 1 is the original damping coefficients obtained from the Angguna car experimental data.

		Csplus (Ns/m)		
		350	2000	4000
Csmin (Ns/m)	1430	Combination 1	Combination 2	Combination 3
	2000	Combination 4	Combination 5	Combination 6
	4000	Combination 7	Combination 8	Combination 9

Fig.4.7 Combinations of the Variations of Damping Coefficients For Both Compressive and Expansive Motion

These combinations of variations of damping coefficients can be summarised in Table 4.1 below to include the asymmetry ratio and the asymmetry average. The asymmetry ratio β is defined as c_s^+/c_s^- while the asymmetry average α is defined as $c_s^+ + c_s^-/2$.

Table 4.1 Combinations of Variations of Damping Coefficients with Their Asymmetry Ratios and Averages

Combination	C_s^+ (Ns/m)	C_s^- (Ns/m)	β	α
1	350	1430	0.24	890
2	2000	1430	1.40	1715
3	4000	1430	2.80	2715
4	350	2000	0.18	1175
5	2000	2000	1.00	2000
6	4000	2000	2.00	3000
7	350	4000	0.09	2175
8	2000	4000	0.50	3000
9	4000	4000	1.00	4000

4.4.2 Modelling Parameters

All parameters used are representatives of a medium passenger car. These parameters are summarised in Table 4.2 below. The damping coefficient of the suspension is a variable and is explained above.

Table 4.2 Parameters of a Medium Passenger Car

Modelling Elements	Symbol	Value	Unit
Mass of Unsprung	M_u	227.55	Kg
Stiffness of Unsprung	K_u	202230	N/m
Damping Coefficient of Unsprung	C_u	6.860	Ns/m
Mass of Sprung	M_s	1794.4	Kg
Stiffness of Sprung	K_s	85439.4	N/m

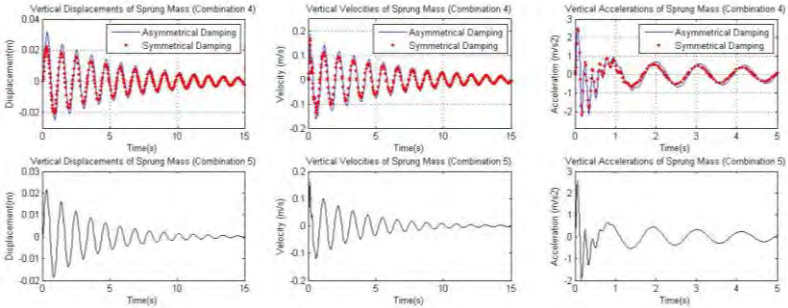

Fig. 5.18 Time Responses of the Asymmetrical and Symmetrical Systems for Combination 4 and 5 Due To Modified Bump Input

Figure 5.18 shows the time responses of the asymmetrical and symmetrical systems for combination 4 and 5 due to modified bump input. Combination 5 has an asymmetry ratio γ value of 1 thus it is already a symmetrical system.

Table 5.10 summarised the maximum responses and their settling times for both asymmetrical and symmetrical systems of combination 4 and 5. For combination 4, the values in the table consistently show that the symmetrical system has a smoother and more progressive performance than the asymmetrical system i.e. lower overshoots. Therefore, we conclude that with modified bump input, the symmetrical system of combination 4 is better than its asymmetrical system.

Table 5.10 Maximum Displacements, Velocities and Accelerations and Settling Times for Both Asymmetrical and Symmetrical Systems of Combination 4 and 5 Due To Modified Bump Input

Responses	Combination		
	4		5
	Asym	Sym	Sym
Maximum Displacement (m)	0.0318	0.0225	0.0217
Settling Time (s)	24.4486	24.9915	14.5751
Maximum Velocity (m/s)	0.1891	0.1672	0.1636
Settling Time (s)	23.6558	23.5407	13.7341
Maximum Acceleration (m/s²)	2.5645	2.4421	2.5754
Settling Time (s)	18.9876	18.8524	10.1523

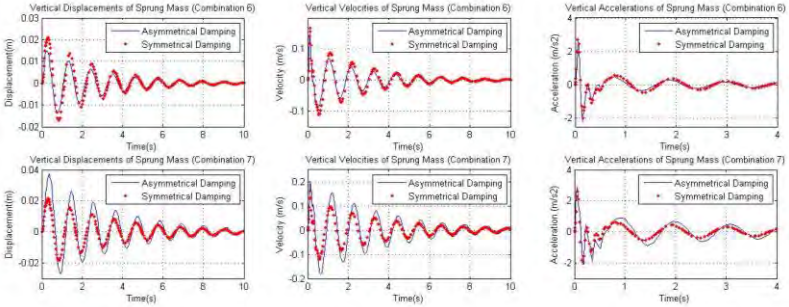

Fig. 5.19 Time Responses of the Asymmetrical and Symmetrical Systems for Combination 6 and 7 Due To Modified Bump Input

Figure 5.19 shows the time responses of the asymmetrical and symmetrical systems for combination 6 and 7 due to modified bump input. Table 5.11 summarised the maximum responses and their settling times for both asymmetrical and symmetrical systems of combination 6 and 7.

For combination 6, the values in the table consistently show that the asymmetrical system has a smoother and more progressive performance than the symmetrical system i.e. lower overshoots. While the values for combination 7 show that actually the symmetrical system has a smoother and more progressive performance instead. Therefore, we conclude that with modified bump input, the asymmetrical system of combination 6 is better than its symmetrical system while the symmetrical system of combination 7 is better than its asymmetrical system.

Table 5.11 Maximum Displacements, Velocities and Accelerations and Settling Times for both Asymmetrical and Symmetrical Systems of Combination 6 and 7 Due To Modified Bump Input

Responses	Combination			
	6		7	
	Asym	Sym	Asym	Sym
Maximum Displacement (m)	0.0147	0.0209	0.0374	0.0216
Settling Time (s)	10.0561	9.6613	13.5523	13.4752
Maximum Velocity (m/s)	0.1534	0.1677	0.2015	0.1636
Settling Time (s)	8.6685	8.8322	13.7955	12.6284
Maximum Acceleration (m/s^2)	2.5739	2.6777	2.8914	2.5938
Settling Time (s)	6.2421	6.3694	10.2104	9.083

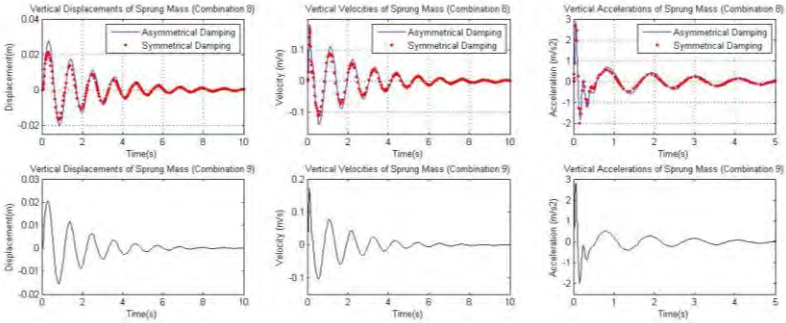

Fig. 5.20 Time Responses of the Asymmetrical and Symmetrical Systems for Combination 8 and 9 Due To Modified Bump Input

Figure 5.20 shows the time responses of the asymmetrical and symmetrical systems for combination 8 and 9 due to modified bump input. Combination 9 has an asymmetry ratio γ value of 1 thus it is already a symmetrical system.

Table 5.12 summarised the maximum responses and their settling times for both asymmetrical and symmetrical systems of combination 8 and 9. For combination 8, the values in the table consistently show that the symmetrical system has a smoother and more progressive performance than the asymmetrical system. Therefore, we conclude that with modified bump input, the symmetrical system of combination 8 is better than its asymmetrical system.

Table 5.12 Maximum Displacements, Velocities and Accelerations and Settling Times for Both Asymmetrical and Symmetrical Systems of Combination 8 and 9 Due To Modified Bump Input

Responses	Combination		
	8		9
	Asym	Sym	Sym
Maximum Displacement (m)	0.0277	0.0209	0.0205
Settling Time (s)	9.6544	9.6613	7.4386
Maximum Velocity (m/s)	0.1805	0.1677	0.1716
Settling Time (s)	9.3864	8.8322	6.6159
Maximum Acceleration (m/s^2)	2.8854	2.6777	2.7783
Settling Time (s)	6.9231	6.3694	4.703

The results obtained with the modified bump input as shown in Figure 5.17-20 and Table 5.9-12 indicate that with increasing damping coefficient average, the overshoot responses and the settling times are lower for all combinations.

It can also be concluded that with modified bump input, combination 2, 3 and 6 provide better damping i.e. lower overshoots when they are asymmetrical systems, while combination 4, 7 and 8 provide better damping when they are symmetrical systems. Combination 5 and 9 are already symmetrical.

Upon investigating the displacement overshoots of all combinations, it is found that combination 3 has the lowest overshoots. This is followed by combination 6 then 2 then 9, 5, 8 and 1. Combination 7 has the highest overshoot while combination 4 the second highest.

5.3.3 Sinusoidal Input

These are the results obtained with the sinusoidal input for the rest of the combination of damping coefficients for asymmetrical and symmetrical damping as shown in Figure 5.21-24.

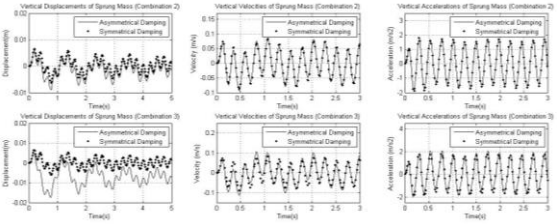

Fig. 5.21 Time Responses of the Asymmetrical and Symmetrical Systems for Combination 2 and 3 Due To Sinusoidal Input

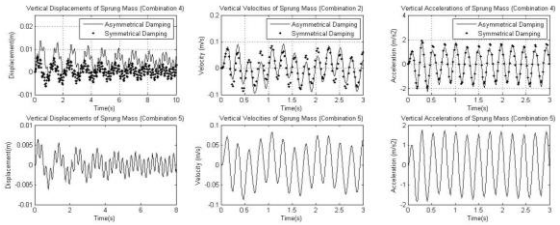

Fig. 5.22 Time Responses of the Asymmetrical and Symmetrical Systems for Combination 4 and 5 Due To Sinusoidal Input

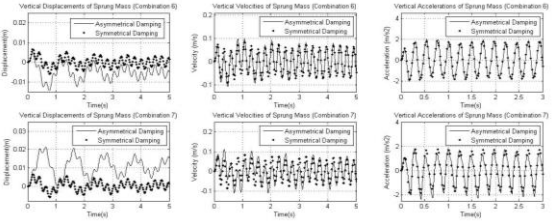

Fig. 5.23 Time Responses of the Asymmetrical and Symmetrical Systems for Combination 6 and 7 Due To Sinusoidal Input

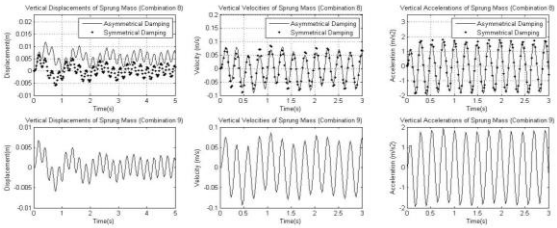

Fig. 5.24 Time Responses of the Asymmetrical and Symmetrical Systems for Combination 8 and 9 Due To Sinusoidal Input

5.4 Evaluations of Ride Comfort

In this section, the combinations of damping coefficients used for simulation are according to Table 4.1. For the symmetrical system, the average of the original damping coefficients (asymmetry average, α) is used. Ride comfort is evaluated for each combination on the different road excitations. For the transient excitations i.e. modified step and bump input, the performance indices are used as measurement of the ride comfort. Meanwhile for the steady state excitation i.e. sinusoidal input, the root-mean-square accelerations of the sprung mass is used as measurement. The influences of the asymmetry ratio (β) and the asymmetry average (α) are also analysed as well as the influence of severity parameter or vehicle velocity.

5.4.1 Modified Step Input

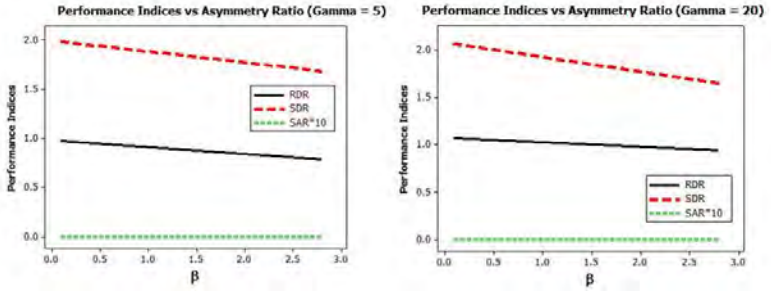

(a) **(b)**

Fig. 5.25 Performance Indices With Respect To Asymmetry Ratio with Severity Parameter of (a) 5 and (b) 20 Due To Modified Step Input

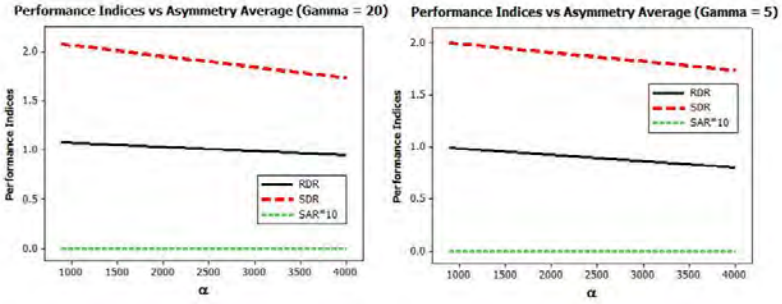

(a) **(b)**

Fig. 5.26 Performance Indices With Respect To Asymmetry Average with Severity Parameter of (a) 5 and (b) 20 Due To Modified Step Input

After simulating all combination of damping coefficients, graphs of performances indices-asymmetry ratio and average are produced to assess its influence on the apparent improvement in comfort provided by the asymmetrical system. Two types of impact are used in this simulation: less severe impact ($\gamma = 5$) and more severe impact ($\gamma = 20$).

Both Figure 5.25 and 5.26 show that using the modified step input, both RDR and SDR are decreasing with increasing asymmetry ratio while the SAR does not

show relatively significant changes in both graphs. At higher value of severity parameter, all values are generally higher.

However the two dimensional graphs are not sufficient to give a good understanding of this. Therefore, three-dimensional graphs are produced to give a better understanding of the influences of both asymmetry ratio and asymmetry average on the performance indices as shown in Figure 5.27.

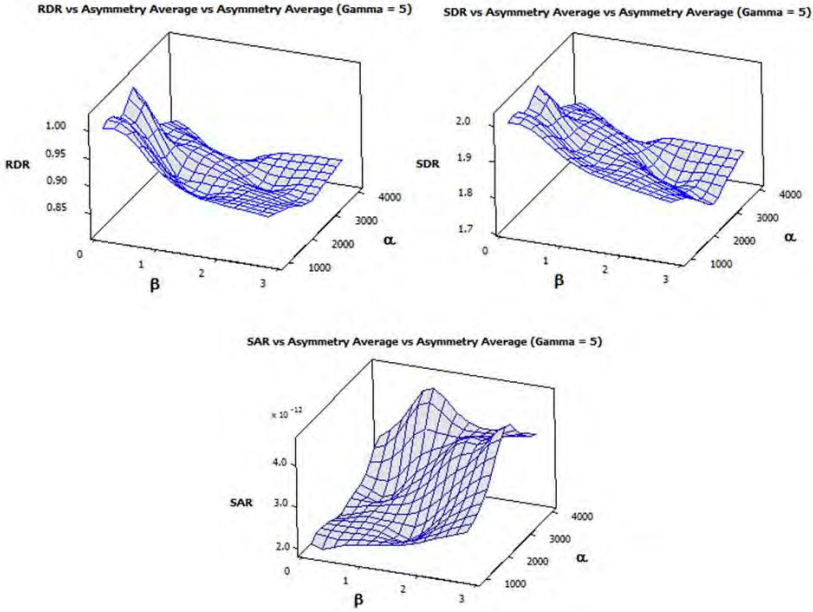

Fig. 5.27 Three Dimensional Graphs of Performance Indices With Respect To Asymmetry Ratio and Average Due To Modified Step Input

As you can see in Figure 5.27, at severity parameter of 5 and with increasing asymmetry ratio and average, both the values of RDR and SDR are decreasing. This is likely due to higher asymmetry ratio and average leads to higher damping and thus lower transmitted displacement

responses (lower SDR values) and smaller strokes (lower RDR values with SDR values above 1). The decrease in the RDR shows that the higher acceleration levels (higher SAR values) are related to smaller relative displacements. Furthermore the values of SAR are almost 0 due to the high values of $\ddot{z_o}$ (around 10^{13} m/s^2).

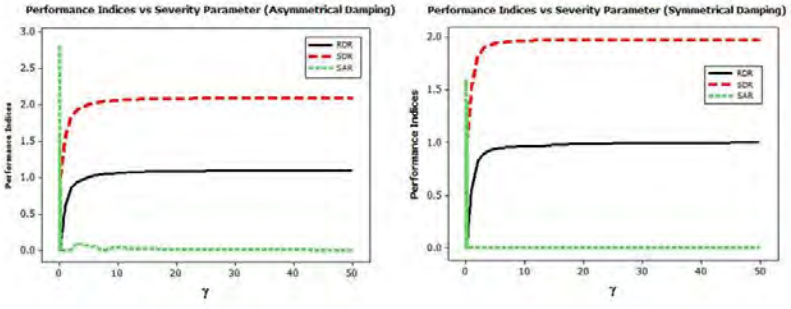

(a) **(b)**

Fig. 5.28 Performance Indices with Respect To Severity Parameter For (a) Asymmetrical and (b) Symmetrical Systems of Combination 1 Due To Modified Step Input

Figure 5.28 above shows the performance indices RDR, SDR and SAR for varying severity parameter γ for the modified step input for the asymmetrical and symmetrical systems for combination 1. Combination 1 has an asymmetry ratio of 0.24, and along with combination 4, 7 and 8, its symmetrical system has performed better than the asymmetrical according to the time responses i.e. lower displacement.

Figure 5.28 shows that both systems perform similarly at lower impacts. However, with more severe impacts, the symmetrical system presents lower indices, indicating smoother behaviour. For example, at γ = 20, the RDR index is 10.19% higher for the asymmetrical the SDR index is 5.94% higher, and the SAR index however is significantly higher since even lower impacts.

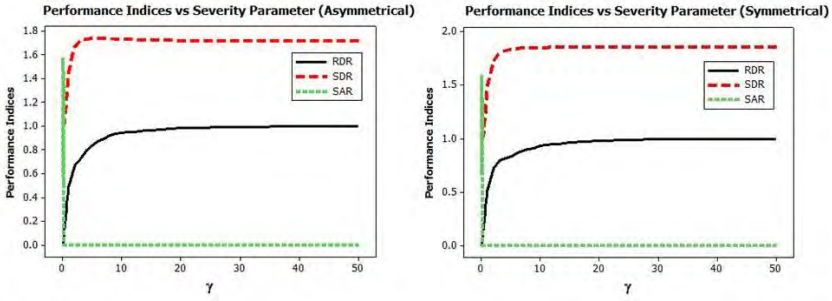

(a) **(b)**

Fig. 5.29 Performance Indices with Respect To Severity Parameter For (a) Asymmetrical and (b) Symmetrical Systems of Combination 3 Due To Modified Step Input

Figure 5.29 above shows the performance indices RDR, SDR and SAR for varying severity parameter γ for the modified step input for the asymmetrical and symmetrical systems for combination 3. Combination 3 has an asymmetry ratio of 2.80, and along with combination 2 and 6, its asymmetrical system has performed better than the symmetrical according to the time responses i.e. lower displacement and delay.

The figures above show that both systems perform similarly at lower impacts. However, with more severe impacts, the asymmetrical system presents lower indices, indicating smoother behaviour. For example, at $\gamma = 20$, the RDR index is 0.61% higher for the asymmetrical the SDR index is 7.23% lower, and the SAR index is 82.65% lower.

The increase in the RDR shows that the lower acceleration levels are related to larger relative displacements, or stroke, between the two blocks. This is a direct consequence of the use of asymmetrical dampers, which provide less damping force on the system on the compression half-cycle, resulting in larger stroke. It is interesting to note that the larger relative displacement

between the unsprung and sprung masses does not necessarily result in larger absolute displacement of the sprung mass.

5.4.2 Modified Bump Input

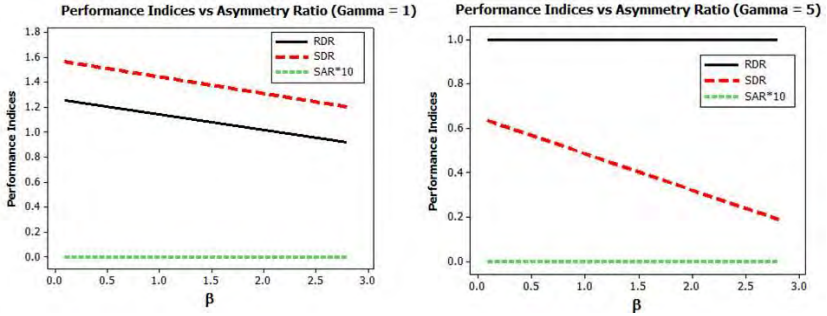

(a) **(b)**

Fig. 5.30 Performance Indices with Respect To Asymmetry Ratio with Severity Parameter of (a) 1 and (b) 5 Due To Modified Bump Input

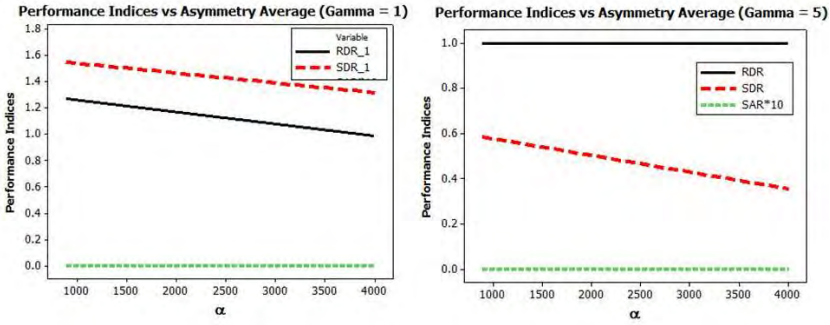

(a) **(b)**

Fig. 5.31 Performance Indices with Respect To Asymmetry Average with Severity Parameter of (a) 1 and (b) 5 Due To Modified Bump Input

After simulating all combination of damping coefficients, graphs of performances indices-asymmetry ratio and average are produced to assess its influence on the apparent improvement in comfort provided by the

asymmetrical system. Two types of impact are used in this simulation: low impact ($\gamma = 1$) and less severe impact ($\gamma = 5$).

Figure 5.30 and 5.31 show the results of these performance indices using the modified step input. For low impact, both RDR and SDR are decreasing with increasing asymmetry ratio. For higher impact though the SDR index is still decreasing however the RDR index has stabilised at 1.0. The SAR index does not show relatively significant changes in both graphs.

However the two dimensional graphs are not sufficient to give a good understanding of this. Therefore, three-dimensional graphs are produced to give a better understanding of the influences of both asymmetry ratio and asymmetry average on the performance indices.

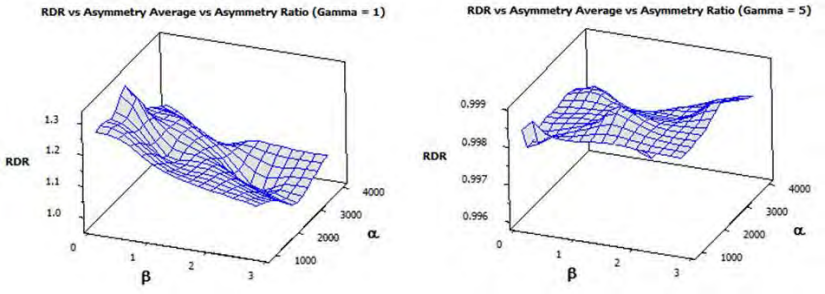

(a) **(b)**

Fig. 5.32 Indices RDR with Respect To Asymmetry Ratio and Average with Severity Parameter of (a) 1 and (b) 5 Due To Modified Bump Input

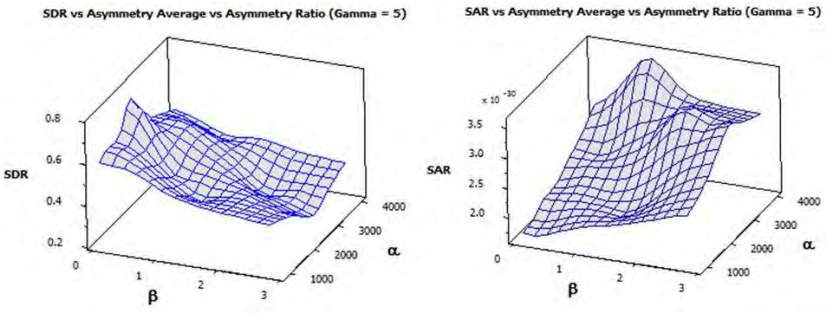

(a) **(b)**

Fig. 5.33 Indices (a) SDR and (b) SAR with Respect To Asymmetry Ratio and Average with Severity Parameter of 5 Due To Modified Bump Input

As you can see in Figure 5.32-33, at severity parameter of 5 and with increasing asymmetry ratio and average, the values of SDR are decreasing but the RDR index has stabilised. If we consider the RDR index at low impact ($\gamma = 1$), we can see that the RDR index is decreasing with increasing asymmetry ratio and average. However as we see in Figure 5.33(b) with increasing asymmetry ratio and average, the value of SAR is increasing instead.

This is likely due to higher asymmetry ratio and average leads to higher damping and thus lower transmitted displacement responses (lower SDR values) and smaller strokes (lower RDR values). The decrease in the RDR shows that the higher acceleration levels (higher SAR values) are related to smaller relative displacements. Furthermore the values of SAR are almost 0 due to the high values of $\ddot{z_o}$.

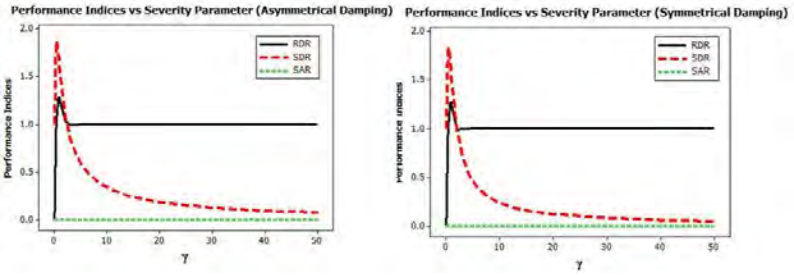

(a) **(b)**

Fig. 5.34 Performance Indices with Respect To Severity Parameter for (a) Asymmetrical and (b) Symmetrical Systems of Combination 1 Due To Modified Bump Input

Figure 5.34 above shows the performance indices RDR, SDR and SAR for varying severity parameter γ for the modified bump input for the asymmetrical and symmetrical systems for combination 1. Combination 1 has an asymmetry ratio of 0.24, and along with combination 4, 7 and 8, its symmetrical system has performed better than the asymmetrical according to the time responses i.e. lower displacement and delay.

The figures above show that with the exception of the SDR index both systems perform similarly at higher impacts. However, with lower impacts, the asymmetrical system presents lower indices, indicating smoother behaviour. For example, at $\gamma = 3$, the RDR index is 0.24% lower for the asymmetrical the SDR index is 16.99% higher, and the SAR index is 1.12% lower.

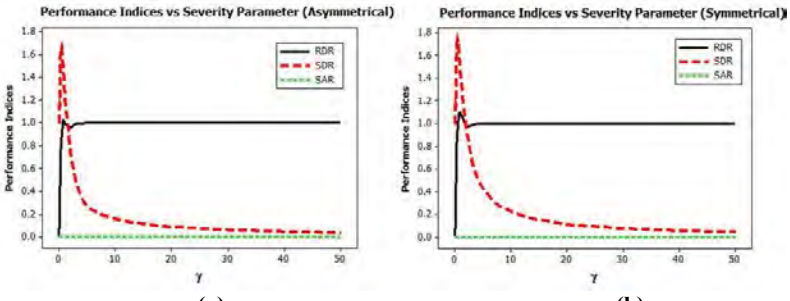

(a) **(b)**

Fig. 5.35 Performance Indices with Respect To Severity Parameter for (a) Asymmetrical and (b) Symmetrical Systems of Combination 3 Due To Modified Bump Input

Figure 5.35 above shows the performance indices RDR, SDR and SAR for varying severity parameter γ for the modified bump input for the asymmetrical and symmetrical systems for combination 3. Combination 3 has an asymmetry ratio of 2.80, and along with combination 2 and 6, its asymmetrical system has performed better than the symmetrical according to the time responses i.e. lower displacement and delay.

Figure 5.35 shows that with the exception of the SDR index both systems perform similarly at higher impacts. However, with lower impacts, the asymmetrical system presents lower indices, indicating smoother behaviour. For example, at $\gamma = 3$, the RDR index is 1.01% higher for the asymmetrical the SDR index is 28.24% lower, and the SAR index is 23.40% higher.

The increase in the RDR shows that the lower acceleration levels are related to larger relative displacements, or stroke, between the two blocks. This is a direct consequence of the use of asymmetrical dampers, which provide less damping force on the system on the compression half-cycle, resulting in larger stroke. It is interesting to note that the larger relative displacement

between the unsprung and sprung masses does not necessarily result in larger absolute displacement of the sprung mass.

5.4.3 Sinusoidal Input

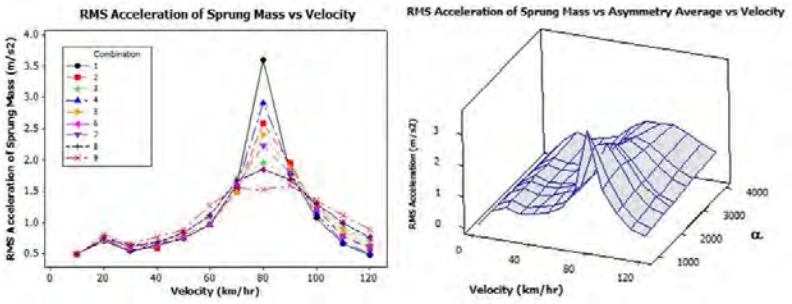

(a) **(b)**

Fig. 5.36 RMS Acceleration of Sprung Mass with Respect To (a) Velocity and (b) Velocity and Asymmetry Average Due To Sinusoidal Input

After simulating all combination of damping coefficients, graphs of root-mean-square acceleration of sprung mass – velocity are produced to assess its influence on the apparent improvement in comfort provided by the asymmetrical system. Figure 5.36(a) above shows that for each combination, RMS acceleration of sprung mass is the highest at velocity of 80 km/hr. We notice that at velocity of 80 km/hr, all combinations reach their highest values of root-mean-square acceleration. Thus we can conclude that at velocity 80 km/hr, resonances happen for all combinations. Combination 1 has the highest RMS acceleration value and combination 9 has the lowest of RMS acceleration. This corresponds to the value of the asymmetry average of the combinations. The three-dimensional graph in Figure 5.36(b) shows the influence of asymmetry average on the RMS acceleration of sprung mass at all velocities.

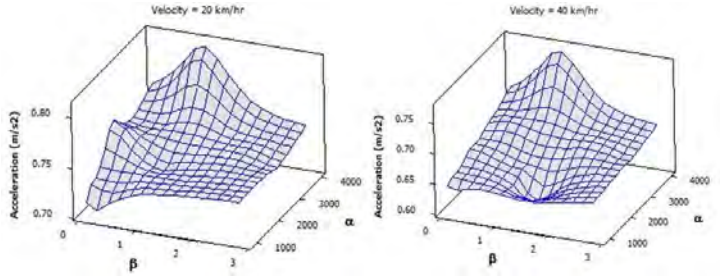

(a) **(b)**

Fig. 5.37 RMS Acceleration of Sprung Mass With Respect To Velocity and Asymmetry Average Due To Sinusoidal Input for Velocity (a) 20 km/hr and (b) 40 km/hr

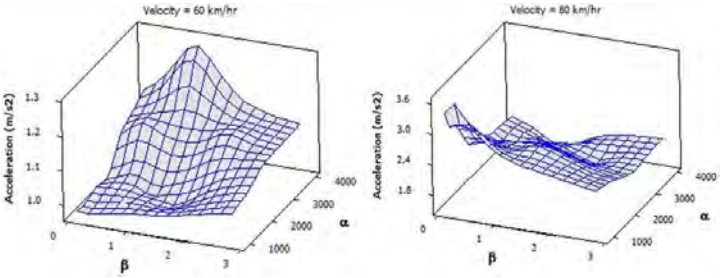

(a) **(b)**

Fig. 5.38 RMS Acceleration of Sprung Mass With Respect To Velocity and Asymmetry Average Due To Sinusoidal Input for Velocity (a) 60 km/hr and (b) 80 km/hr

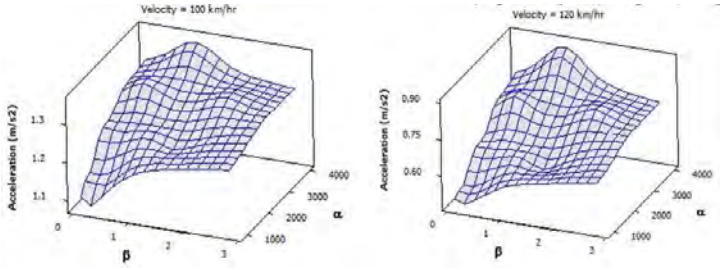

(a) **(b)**

Fig. 5.39 RMS Acceleration of Sprung Mass With Respect To Velocity and Asymmetry Average Due To Sinusoidal Input for Velocity (a) 100 km/hr and (b) 120 km/hr

The graphs in Figure 5.37-39 show that the RMS accelerations values with respect to asymmetry ratio and average at different velocities – 20, 40, 60, 80, 100 and 120 km/hr. There is a similar trend with the RMS acceleration of sprung mass with respect to asymmetry ratio and average for all velocities except at 80 km/hr, which is the velocity at which resonance happens. This trend shows a higher RMS acceleration of sprung mass values with increasing asymmetry average, while the asymmetry ratio is a relatively insignificant factor.

However at velocity 80 km/hr as shown in Figure 5.38(b), the graph shows a completely different trend. At the resonant velocity, the RMS acceleration of sprung mass decreases with increasing value of asymmetry average.

The highest RMS acceleration values are at velocity of 80 km/hr row with 3.60 m/s^2 being the highest for combination 1. According to Table 2.1 this value is classed as extremely uncomfortable. Not only combination 1, combination 2,4,5 and 7 are also classed as extremely uncomfortable at velocity 80 km/hr. Combination 3,6 and 8 are classed as very uncomfortable while combination 9 is classed as uncomfortable.

According to Figure 2.6 with combination 1 at vehicle velocity of 80 km/hr, passengers can keep riding only for less than 1 minute before exhaustion. With combination 2, 4 and 5 at 80 km/hr, passengers can keep riding for about 1 minute. With combination 3 and 7, passengers can keep riding for about 16 minutes. With combination 6 and 8, passengers can keep riding for about 25 minutes, while with combination 9, passengers can keep riding up until just about 1 hour.

CHAPTER V
ANALYSIS OF RESULTS

5.1 Time Responses Modelling

This section contains the time responses of the quarter car model with the original damping coefficients in which c_s^+ is 350 Ns/m and c_s^- is 1430 Ns/m of which make up combination 1. The road excitations inputted into the system modelling are the modified step input, modified bump input and the sinusoidal input.

5.1.1 Modified Step Input

The following graphics shown in Figure 5.1-3 are the displacement, velocity and acceleration time responses produced for both the sprung and unsprung mass due to the modified step input.

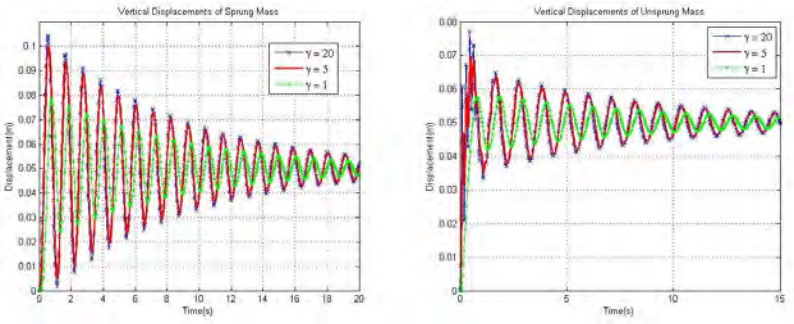

(a) **(b)**

Fig. 5.1 Vertical Displacement-Time Responses of (a) Sprung Mass and (b)Unsprung Mass Due To Modified Step Input

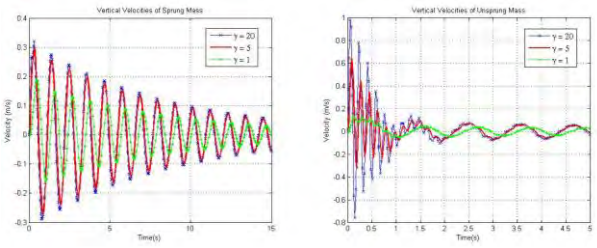

(a) **(b)**

Fig. 5.2 Vertical Velocity-Time Responses of (a) Sprung Mass and (b)Unsprung Mass Due To Modified Step Input

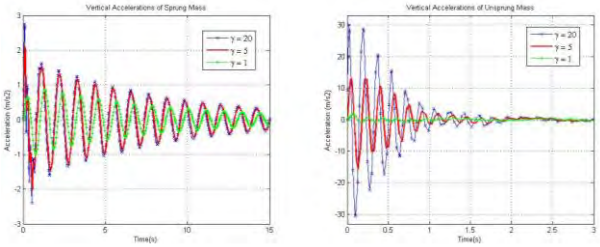

(a) **(b)**

Fig. 5.3 Vertical Acceleration-Time Responses of (a) Sprung Mass and (b)Unsprung Mass Due To Modified Step Input

There are three variations of severity parameter γ in the graphics i.e. 1 for low impact, 5 for less severe impact and 20 for more severe impact. With modified step input, the increase in severity parameter leads to increasing overshoots and settling times for both the sprung and unsprung masses i.e. for sprung mass at γ value of 1, the maximum displacement is 0.08 m and the settling time is 28.65s while at γ value of 5, the maximum displacement is 0.10 m and the settling time is 33.39 s.

It is also observed that overshoots and settling times for sprung masses are higher than for unsprung masses. Table 5.1 summarises the maximum responses as well as

the settling time for each response for different value of severity parameter.

Table 5.1 Maximum Displacements, Velocities and Accelerations for Both Masses at Different Severity Parameters Due To Modified Step Input

Responses	Sprung Mass			Unsprung Mass		
	γ = 1	γ = 5	γ = 20	γ = 1	γ = 5	γ = 20
Maximum Displacement (m)	0.08	0.10	0.10	0.06	0.07	0.08
Settling Time (s)	28.65	33.39	33.34	18.32	23.59	24.06
Maximum Velocity (m/s)	0.19	0.30	0.32	0.13	0.65	0.99
Settling Time (s)	32.21	33.11	32.54	57.62	22.12	14.48
Maximum Acceleration(m/s^2)	1.00	2.09	2.76	1.74	15.71	30.55
Settling Time (s)	33.55	32.23	30.09	N/A	8.24	2.75

5.1.2 Modified Bump Input

The following graphics shown in Figure 5.4-6 are the displacement, velocity and acceleration time responses produced for both the sprung and unsprung mass due to the modified bump input.

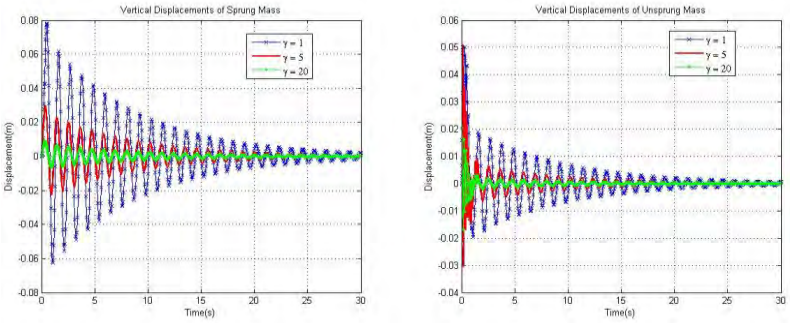

(a) **(b)**

Fig. 5.4 Vertical Displacement-Time Responses of (a) Sprung Mass and (b) Unsprung Mass Due To Modified Bump Input

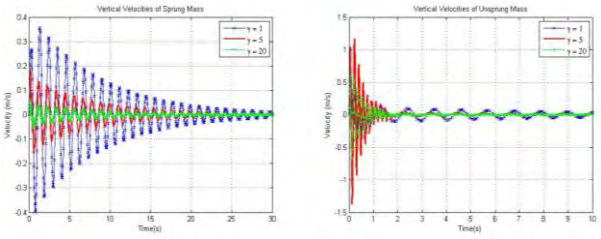

(a) **(b)**

Fig. 5.5 Vertical Velocity-Time Responses of (a) Sprung Mass and (b) Unsprung Mass Due To Modified Bump Input

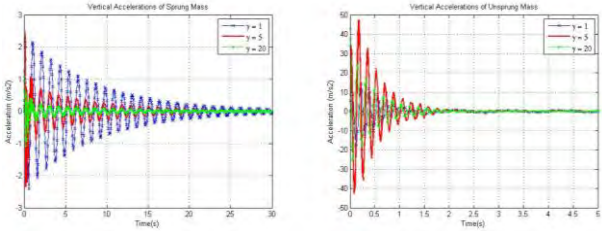

(a) **(b)**

Fig. 5.6 Vertical Acceleration-Time Responses of (a) Sprung Mass and (b) Unsprung Mass Due To Modified Bump Input

There are three variations of severity parameter γ in the graphics i.e. 1 for low impact, 5 for less severe impact and 20 for more severe impact. With modified bump input, the increase in severity parameter leads to decreasing overshoots and settling times for both the sprung and unsprung masses i.e. for sprung mass at γ value of 1, the maximum displacement is 0.08 m and the settling time is 32.21 s while at γ value of 5, the maximum displacement is 0.03 m and the settling time is 32.10 s.

It is also observed that overshoots and settling times for sprung masses are higher than for unsprung masses.. Table 5.2 summarises the maximum responses as well as the settling time for each responses.

Table 5.2 Maximum Displacements, Velocities and Accelerations for Both Masses at Different Severity Parameters Due To Modified Bump Input

Responses	Sprung Mass			Unsprung Mass		
	γ = 1	γ = 5	γ = 20	γ = 1	γ = 5	γ = 20
Maximum Displacement (m)	0.08	0.03	0.01	0.05	0.05	0.02
Settling Time (s)	32.21	32.10	31.01	25.65	17.79	16.70
Maximum Velocity (m/s)	0.40	0.18	0.06	0.67	1.37	0.67
Settling Time (s)	33.54	30.74	29.09	20.32	4.96	2.32
Maximum Acceleration (m/s^2)	2.41	2.52	1.08	17.28	47.30	42.56
Settling Time (s)	33.33	24.41	21.19	11.42	1.95	1.65

5.1.3 Sinusoidal Input

The following graphics shown in Figure 5.7-9 are the displacement, velocity and acceleration time responses produced for both the sprung and unsprung mass due to the sinusoidal input. With increasing velocity, the displacement, velocity and acceleration responses of both masses also increase. The displacement of sprung mass at velocity 80 km/hr is quite high that the vehicle can be said partially airborne.

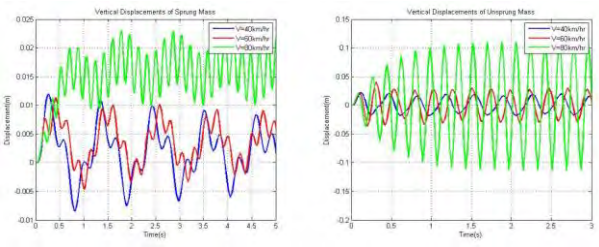

(a) **(b)**

Fig. 5.7 Vertical Displacement-Time Responses of (a) Sprung Mass and (b) Unsprung Mass Due To Sinusoidal Input

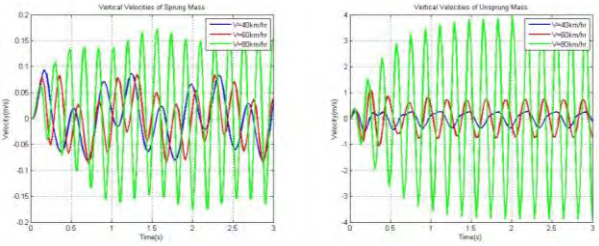

(a) **(b)**

Fig. 5.8 Vertical Velocity-Time Responses of (a) Sprung Mass and (b) Unsprung Mass Due To Sinusoidal Input

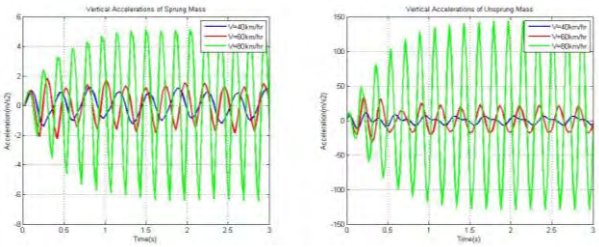

(a) **(b)**

Fig. 5.9 Vertical Acceleration-Time Responses of (a) Sprung Mass and (b) Unsprung Mass Due To Sinusoidal Input

5.2 Asymmetrical and Symmetrical Time Responses Modelling

This section contains a comparison between two quarter-car system - one in which c_s is symmetrical and another in which c_s is asymmetrical. The graphics obtained for this section is only of the sprung mass. The original damping coefficients in which c_s^+ is 350 Ns/m and c_s^- is 1430 Ns/m (Combination 1) are used for the asymmetrical system. For the symmetrical system, the average of the original damping coefficients (asymmetry average, α = 890 Ns/m) is used. The road excitations used are the modified step and bump input, and the sinusoidal input.

5.2.1 Modified Step Input

The following graphics shown in Figure 5.10 are the displacement, velocity and acceleration time responses produced for both the asymmetrical and symmetrical systems of combination 1 due to the modified step input.

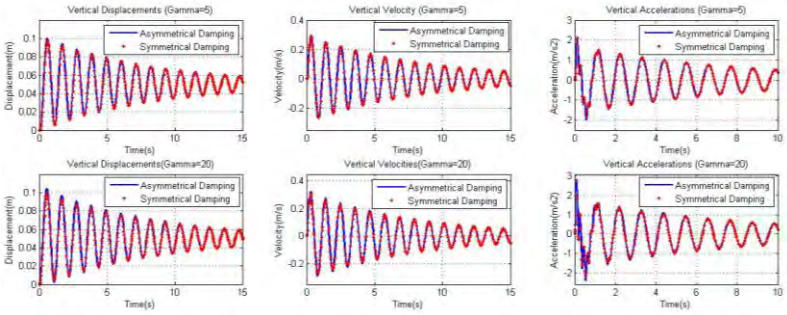

Fig. 5.10 Time Responses of the Asymmetrical and Symmetrical Systems with Different Severity Parameters Due To Modified Step Input

The results obtained with the modified step input as shown in Figure 5.10 indicate that at both types of impact (γ = 5 and 20), the two systems present similar behaviour to each other with the symmetrical system being slightly

superior i.e. at $\gamma = 5$ the asymmetrical system has a maximum displacement of 0.1001 m and settling time of 33.3907 s while the symmetrical system has a lower displacement of 0.0968 m and shorter settling time of 32.8512 s.

Table 5.3 summarises the maximum responses and their settling times for both asymmetrical and symmetrical systems at both types of impact. The values in the table consistently show that the symmetrical system has a smoother and more progressive performance than the asymmetrical system i.e. the maximum responses and settling time values are lower. Therefore, we conclude that with modified step input and combination 1 as damping coefficients, the symmetrical system is better than the asymmetrical system at both types of impact.

Table 5.3 Maximum Displacements, Velocities and Accelerations For Both Asymmetrical and Symmetrical Systems of Combination 1 at Two Types of Impact ($\gamma = 5$ and 20) Due To Modified Step Input

Responses	$\gamma = 5$		$\gamma = 20$	
	Asym	Sym	Asym	Sym
Maximum Displacement (m)	0.1001	0.0968	0.1043	0.0984
Settling Time (s)	33.3907	32.8512	33.357	32.8118
Maximum Velocity (m/s)	0.2974	0.2882	0.3215	0.305
Settling Time (s)	33.1086	33.0751	32.5392	32.5214
Maximum Acceleration (m/s^2)	2.0931	2.1291	2.7629	2.8069
Settling Time (s)	32.237	31.1896	30.098	29.0121

5.2.2 Modified Bump Input

The following graphics shown in Figure 5.11 are the displacement, velocity and acceleration time responses produced for both the asymmetrical and symmetrical systems of combination 1 due to the modified bump input.

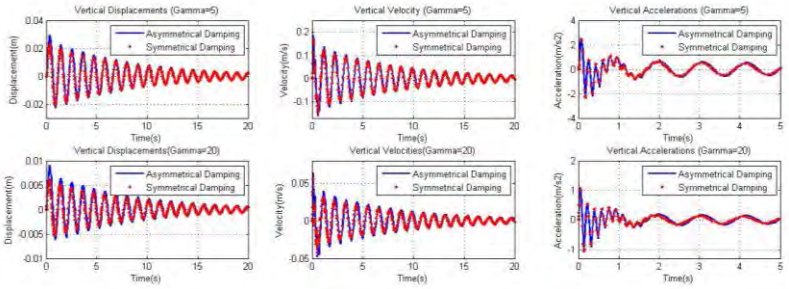

Fig. 5.11 Time Responses of the Asymmetrical and Symmetrical Systems with Different Severity Parameters Due To Modified Bump Input

The results obtained with the modified bump input as shown in Figure 5.11 indicate that at both types of impact ($\gamma = 5$ and 20), the two systems present similar behaviour to each other with the symmetrical system being slightly superior i.e. at $\gamma = 5$ the asymmetrical system has a maximum displacement of 0.0295 m and settling time of 32.0877 s while the symmetrical system has a lower displacement of 0.0229 m and shorter settling time of 32.5879 s.

Table 5.4 summarises the maximum responses and their settling times for both asymmetrical and symmetrical systems at both types of impact. The values in the table consistently show that the symmetrical system has a smoother and more progressive performance than the asymmetrical system i.e. the maximum responses is lower. Therefore, we conclude that with modified bump input and combination 1 as damping coefficients, the symmetrical

system is better than the asymmetrical system at both types of impact.

Table 5.4 Maximum Displacements, Velocities and Accelerations for Both Asymmetrical and Symmetrical Systems of Combination 1 at Two Types of Impact (γ = 5 and 20) Due To Modified Bump Input

Responses	γ = 5		γ = 20	
	Asym	Sym	Asym	Sym
Maximum Displacement (m)	0.0295	0.0229	0.0091	0.0061
Settling Time (s)	32.0877	32.5879	31.5712	32.0122
Maximum Velocity (m/s)	0.1845	0.169	0.0637	0.0568
Settling Time (s)	30.7473	31.1906	29.6332	28.9913
Maximum Acceleration (m/s^2)	2.5217	2.4003	1.0822	1.0499
Settling Time (s)	24.4036	23.7795	21.6684	19.4083

5.2.3 Sinusoidal Input

The results obtained with the sinusoidal input as shown in Figure 5.12 indicate that at low speed (velocity of 40 km/hr), the two systems present similar behaviour. With increasing speed (velocity of 80 km/hr), the displacement of Z_s is lower for the symmetrical system than the asymmetrical system however slight. Therefore, we conclude that with sinusoidal input and combination 1 as damping coefficients, the symmetrical system is better than the asymmetrical system.

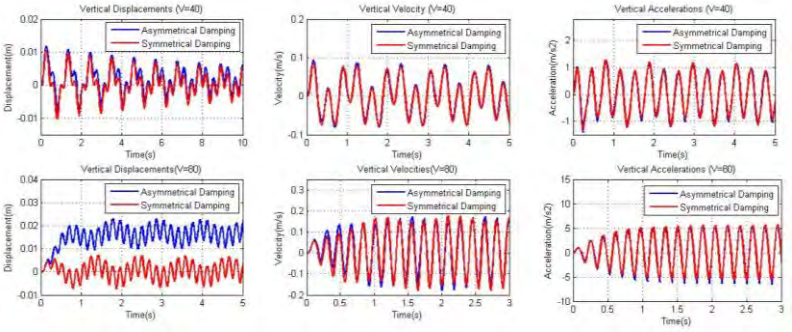

Fig. 5.12 Time Responses of the Asymmetrical and Symmetrical Systems with Different Vehicle Velocities Due To Sinusoidal Input

5.3 Time Responses Modelling with Combinations of Variations of Damping Coefficients

This section contains a comparison between two quarter-car system - one in which c_s is symmetrical and another in which c_s is asymmetrical. The graphics obtained for this section is only of the sprung mass and only for severity parameter value of 5 or velocity of 60 km/hr. The damping coefficients used are varied according to Figure 4.10 as asymmetrical system with exception to combination 1. For the symmetrical system, the average of the original damping coefficients (asymmetry average, α) is used. The exception of combination 5 and 9 are made because they are already symmetrical. The road excitations used are the modified step input, modified bump input and the sinusoidal input.

5.3.1 Modified Step Input

The following graphics shown in Figure 5.13-16 are the displacement, velocity and acceleration time responses produced for both the asymmetrical and symmetrical systems of combination 2 to 9 due to the modified step input.

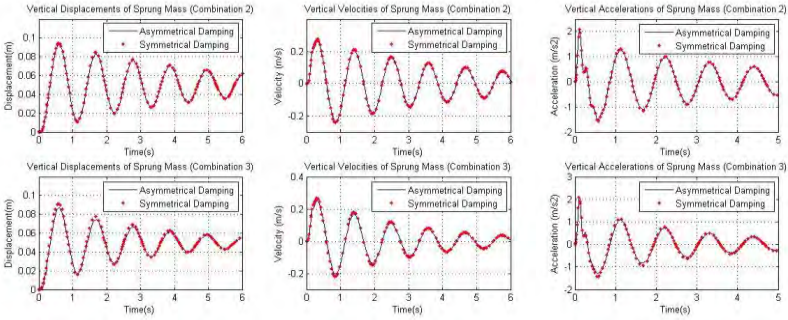

Fig. 5.13 Time Responses of the Asymmetrical and Symmetrical Systems for Combination 2 and 3 Due To Modified Step Input

Figure 5.13 shows the time responses of the asymmetrical and symmetrical systems for combination 2 and 3 due to modified step input. As we can see, the two systems for both combinations present similar behaviour. On investigating their maximum responses and settling time, we found that for combination 2 the asymmetrical system us slightly superior i.e. the asymmetrical system has a maximum displacement of 0.0932 m and settling time of 16.9818 s while the symmetrical system has a higher displacement of 0.0944 m and longer settling time of 17.013 s.

For combination 3 we can also see that the asymmetrical system has a lower maximum displacement and shorter settling time than the symmetrical system i.e. the asymmetrical system has a maximum displacement of 0.0876 m and settling time of 10.4573 s while the symmetrical system has a higher displacement of 0.02516 m and longer settling time of 10.7494 s.

Table 5.5 summarises the maximum responses and their settling times for both asymmetrical and symmetrical systems of combination 2 and 3. For both combinations, the values in the table consistently show that the

asymmetrical system has a smoother and more progressive performance than the symmetrical system i.e. the maximum responses and settling time values are lower. Therefore, we conclude that with modified step input, the asymmetrical systems of both combination 2 and 3 are better than their symmetrical systems.

Table 5.5 Maximum Displacements, Velocities and Accelerations and Settling Times for both Asymmetrical and Symmetrical Systems of Combination 2 and 3 Due To Modified Step Input

Responses	Combination			
	2		3	
	Asym	Sym	Asym	Sym
Maximum Displacement (m)	0.0932	0.0944	0.0867	0.2516
Settling Time (s)	16.9818	17.013	10.4573	10.7494
Maximum Velocity (m/s)	0.2734	17.2625	0.2516	0.2666
Settling Time (s)	17.2395	0.2769	10.7494	10.7437
Maximum Acceleration (m/s^2)	2.0931	2.0961	2.0342	2.098
Settling Time (s)	15.9291	15.9191	9.9376	9.9106

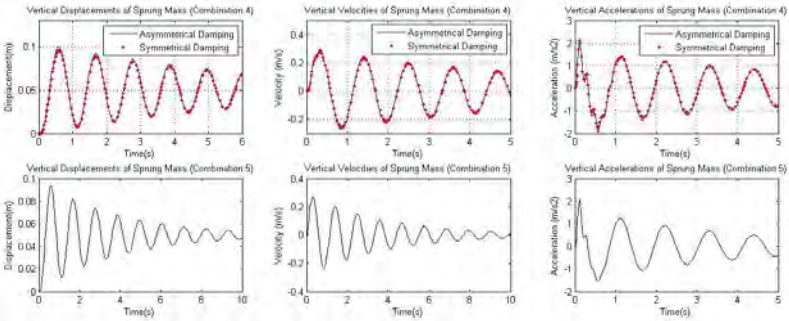

Fig. 5.14 Time Responses of the Asymmetrical and Symmetrical Systems for Combination 4 and 5 Due To Modified Step Input

Figure 5.14 shows the time responses of the asymmetrical and symmetrical systems for combination 4 and 5 due to modified step input. Combination 5 has an asymmetry ratio γ value of 1 thus it is already a symmetrical system.

Table 5.6 summarises the maximum responses and their settling times for both asymmetrical and symmetrical systems of combination 4 and 5. For combination 4, the values in the table consistently show that the symmetrical system has a smoother and more progressive performance than the asymmetrical system i.e. the maximum responses and settling time values are lower. Therefore, we conclude that with modified step input, the symmetrical system of combination 4 is better than its asymmetrical system.

Table 5.6 Maximum Displacements, Velocities and Accelerations and Settling Times for Both Asymmetrical and Symmetrical Systems of Combination 4 and 5 Due To Modified Step Input

Responses	Combination		
	4		5
	Asym	Sym	Sym
Maximum Displacement (m)	0.1005	0.093	0.0936
Settling Time (s)	25.1591	24.6647	14.3099
Maximum Velocity (m/s)	0.2965	0.284	0.274
Settling Time (s)	24.9369	24.9199	14.5653
Maximum Acceleration (m/s^2)	2.0701	2.1149	2.0701
Settling Time (s)	25.7071	23.5636	13.7435

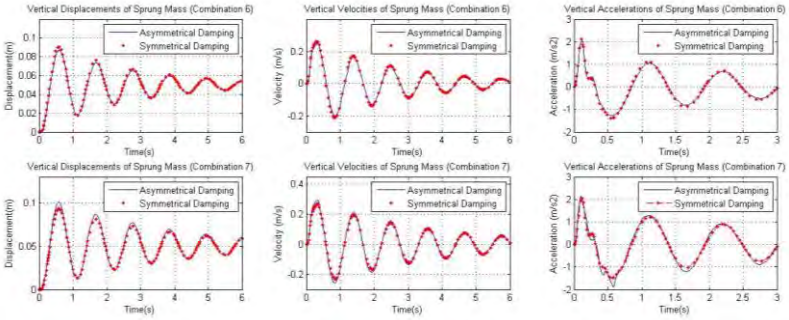

Fig. 5.15 Time Responses of the Asymmetrical and Symmetrical Systems for Combination 6 and 7 Due To Modified Step Input

Figure 5.15 shows the time responses of the asymmetrical and symmetrical systems for combination 6 and 7 due to modified step input, while Table 5.7 summarises the maximum responses and their settling times for both systems of both combinations.

For combination 6, the values in the table consistently show that the asymmetrical system has a smoother and more progressive performance than the symmetrical system i.e. the maximum responses and settling time values are lower. For combination 7, the values in the table consistently show that actually the symmetrical system has a smoother and more progressive performance than the asymmetrical system. Therefore, we conclude that with modified step input, the asymmetrical system of combination 6 is better than its symmetrical system while the symmetrical system of combination 7 is better than its asymmetrical system.

Table 5.7 Maximum Displacements, Velocities and Accelerations and Settling Times for both Asymmetrical and Symmetrical Systems of Combination 6 and 7 Due To Modified Step Input

Responses	Combination			
	6		7	
	Asym	Sym	Asym	Sym
Maximum Displacement (m)	0.0871	0.0909	0.101	0.0931
Settling Time (s)	9.389	9.4056	13.743	13.2128
Maximum Velocity (m/s)	0.2521	0.2644	0.2926	0.2722
Settling Time (s)	9.6635	9.6613	13.4737	13.4708
Maximum Acceleration (m/s^2)	2.0131	2.1184	0.2926	0.2722
Settling Time (s)	8.8323	8.8137	13.4737	13.4708

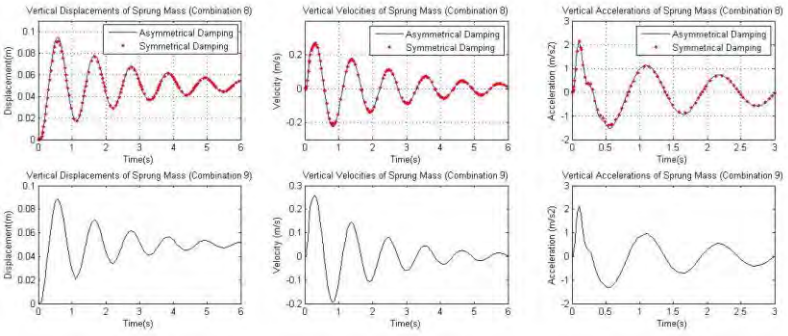

Fig. 5.16 Time Responses of the Asymmetrical and Symmetrical Systems for Combination 8 and 9 Due To Modified Step Input

Figure 5.16 shows the time responses of the asymmetrical and symmetrical systems for combination 8 and 9 due to modified step input. Combination 9 has an asymmetry ratio γ value of 1 thus it is already a symmetrical system.

Table 5.8 summarises the maximum responses and their settling times for both asymmetrical and symmetrical

systems of combination 8 and 9. For combination 8, the values in the table consistently show that the symmetrical system has a smoother and more progressive performance than the asymmetrical system i.e. the maximum responses and settling time values are lower. Therefore, we conclude that with modified step input, the symmetrical system of combination 8 is better than its asymmetrical system.

Table 5.8 Maximum Displacements, Velocities and Accelerations and Settling Times for Both Asymmetrical and Symmetrical Systems of Combination 8 and 9 Due To Modified Step Input

Responses	Combination		
	8		9
	Asym	Sym	Sym
Maximum Displacement (m)	0.0946	0.0909	0.0885
Settling Time (s)	9.8196	9.4056	7.1828
Maximum Velocity (m/s)	0.2758	0.2644	0.2585
Settling Time (s)	9.6504	9.6613	7.4402
Maximum Acceleration (m/s^2)	2.1384	2.1184	2.1347
Settling Time (s)	9.3192	8.8137	6.6425

The results obtained with the modified step input as shown in Figure 5.13-16 and Table 5.4-8 indicate that with increasing damping coefficient average, the overshoot responses and the settling times are lower for all combinations.

It can also be concluded that with modified step input, combination 2, 3 and 6 provide better damping when they are asymmetrical systems, while combination 4, 7 and 8 provide better damping when they are symmetrical systems. Combination 5 and 9 are already symmetrical.

Upon investigating the displacement overshoots of all combinations, it is found that combination 3 and 6 have the lowest overshoots. This is followed by combination 9 then 2 then 5, 8, 1 and lastly 4 and 7.

5.3.2 Modified Bump Input

The following graphics shown in Figure 5.17-20 are the displacement, velocity and acceleration time responses produced for both the asymmetrical and symmetrical systems of combination 2 to 9 due to the modified bump input.

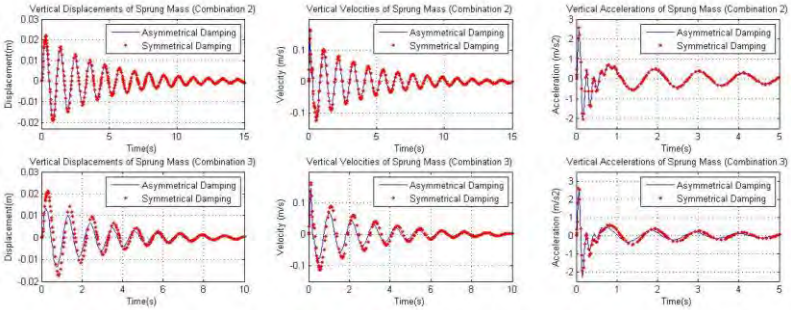

Fig. 5.17 Time Responses of the Asymmetrical and Symmetrical Systems for Combination 2 and 3 Due To Modified Bump Input

Figure 5.17 is the time responses of the asymmetrical and symmetrical systems for combination 2 and 3 due to modified bump input. On investigating their maximum responses and settling time, we found that for combination 2 the asymmetrical system us slightly superior i.e. the asymmetrical system has a maximum displacement of 0.0194 m and settling time of 17.2644 s while the symmetrical system has a higher displacement of 0.0219 m yet shorter settling time of 17.245 s.

For combination 3 we can also see that the asymmetrical system has a lower maximum displacement

yet longer settling time than the symmetrical system i.e. the asymmetrical system has a maximum displacement of 0.0134 m and settling time of 11.6742 s while the symmetrical system has a higher displacement of 0.0212 m and longer settling time of 10.7505 s.

Table 5.9 summarised the maximum responses and their settling times for both asymmetrical and symmetrical systems of combination 2 and 3. For both combinations, the values in the table consistently show that the asymmetrical system has a smoother and more progressive performance than the symmetrical system i.e. lower overshoots. Therefore, we conclude that with modified bump input, the asymmetrical systems of both combination 2 and 3 are better than their symmetrical systems.

Table 5.9 Maximum Displacements, Velocities and Accelerations and Settling Times for Both Asymmetrical and Symmetrical Systems of Combination 2 and 3 Due To Modified Bump Input

Responses	Combination			
	2		3	
	Asym	Sym	Asym	Sym
Maximum Displacement (m)	0.0194	0.0219	0.0134	0.0212
Settling Time (s)	17.2644	17.245	11.6742	10.750
Maximum Velocity (m/s)	0.1574	0.1646	0.1468	0.1664
Settling Time (s)	15.8817	15.9009	9.275	9.9069
Maximum Acceleration (m/s^2)	2.5092	2.5525	2.5181	2.5859
Settling Time (s)	11.8051	11.8224	6.2997	7.421

CHAPTER VI
CONCLUSIONS

The conclusions that can be drawn from this research study are summarised in the following:

1. The results obtained with both the modified step and bump inputs indicate that with increasing damping coefficient average, the overshoot responses and the settling times are lower for all combinations. With modified step input, the better system of the combination always shows lower maximum responses and shorter settling times, consistently. However, with modified bump input, the better system of the combination often shows lower maximum responses yet with longer settling times.
2. With modified step input, it is found that combination 3 and 6 have the lowest overshoots. This is followed by combination 9 then 2 then 5, 8, 1 and lastly 4 and 7. With modified bump input, it is found that combination 3 has the lowest overshoots. This is followed by combination 6 then 2 then 9, 5, 8 and 1. Combination 7 has the highest overshoot while combination 4 the second highest.
3. The results obtained with the transient inputs indicate that combination 2, 3 and 6 (asymmetry ratio β above 1) provide better damping when they are asymmetrical systems while combination 4, 7 and 8 (asymmetry ratio β below 1) provide better damping when they are symmetrical systems. Combination 5 and 9 are already symmetrical.
4. The comparison between the symmetrical and asymmetrical systems under the transient inputs and with the quarter car model showed that the asymmetrical system, with non-linear characteristics and asymmetry ratio above 1, tends to have a smoother and more progressive performance. This tendency increases with larger severity of impacts for the modified step input; meanwhile for the

modified bump input, this happens only for the SDR index while the RDR index stabilised. The asymmetry average also affects the performance of the vehicle. The higher the asymmetry average, the smoother and better the ride comfort.

5. The comparison between the symmetrical and asymmetrical systems under steady-state input i.e. sinusoiral with the quarter car model showed that the asymmetry ratio of the systems does not influence the performance, instead the asymmetry average does. This performance shows the same trend at different velocities except the resonant velocity. At the resonant velocity, the quarter car model shows that the higher the asymmetry average, the higher is the performance of the vehicle. At any other velocity, the quarter car model shows that the performance is lower the higher the asymmetry average.

ENCLOSURE 1

Ride Comfort Evaluation Data For Modified Step Input

1. Performance Indices Generated After Simulating All Combinations at Severity Parameter γ of 1

					Asymmetrical			Symmetrical		
Combination	C_s^+	C_s^-	β	α	RDR	SDR	SAR*10	RDR	SDR	SAR*10
1	350	1430	0.24	890	0.594	1.565	5.19E-17	0.579	1.550	9.76E-14
2	2000	1430	1.40	1715	0.538	1.508	1.84E-13	0.544	1.515	1.78E-13
3	4000	1430	2.80	2715	0.478	1.448	9.64E-14	0.507	1.477	8.36E-14
4	350	2000	0.18	1175	0.589	1.560	5.13E-17	0.567	1.538	6.73E-14
5	2000	2000	1	2000	0.533	1.504	1.82E-13	0.533	1.504	1.82E-13
6	4000	2000	2	3000	0.473	1.444	9.66E-14	0.497	1.466	7.48E-14
7	350	4000	0.09	2175	0.576	1.545	4.99E-17	0.526	1.497	1.89E-13
8	2000	4000	0.5	3000	0.522	1.490	1.78E-13	0.497	1.466	7.48E-14
9	4000	4000	1	4000	0.463	1.433	9.44E-14	0.463	1.433	9.44E-14

2. Performance Indices Generated After Simulating All Combinations at Severity Parameter γ of 5

					Asymmetrical			Symmetrical		
Combination	C_s^+	C_s^-	β	α	RDR	SDR	SAR*10	RDR	SDR	SAR*10
1	350	1430	0.24	890	1.002	2.002	1.95E-12	0.937	1.937	4.06E-12
2	2000	1430	1.40	1715	0.863	1.863	1.95E-12	0.888	1.888	1.69E-12
3	4000	1430	2.80	2715	0.839	1.734	4.51E-12	0.832	1.832	3.57E-12
4	350	2000	0.18	1175	1.010	2.010	2.20E-12	0.919	1.919	1.88E-12
5	2000	2000	1	2000	0.871	1.871	2.20E-12	0.871	1.871	2.20E-12
6	4000	2000	2	3000	0.833	1.741	3.88E-12	0.817	1.817	3.70E-12
7	350	4000	0.09	2175	1.020	2.020	2.01E-12	0.862	1.862	2.54E-12
8	2000	4000	0.5	3000	0.893	1.893	2.01E-12	0.817	1.817	3.70E-12
9	4000	4000	1	4000	0.815	1.770	4.34E-12	0.815	1.771	4.34E-12

3. Performance Indices Generated After Simulating All Combinations at Severity Parameter γ of 20

					Asymmetrical			Symmetrical		
Combination	C_s^+	C_s^-	β	α	RDR	SDR	SAR*10	RDR	SDR	SAR*10
1	350	1430	0.24	890	1.086	2.086	1.70E-10	0.985	1.969	5.48E-11
2	2000	1430	1.40	1715	0.983	1.873	4.39E-11	0.980	1.913	5.45E-11
3	4000	1430	2.80	2715	0.983	1.719	4.53E-11	0.977	1.853	2.52E-10
4	350	2000	0.18	1175	1.105	2.105	8.71E-11	0.984	1.949	5.17E-11
5	2000	2000	1	2000	0.979	1.896	5.03E-11	0.979	1.896	5.03E-11
6	4000	2000	2	3000	0.978	1.739	3.48E-12	0.975	1.840	2.60E-10
7	350	4000	0.09	2175	1.126	2.126	2.89E-10	0.977	1.885	5.70E-11
8	2000	4000	0.5	3000	0.972	1.940	5.95E-11	0.975	1.840	2.60E-10
9	4000	4000	1	4000	0.972	1.787	6.01E-11	0.972	1.787	6.01E-11

4. Performance Indices Generated After Simulating The Asymmetrical System ($\beta = 0.24$) and Symmetrical System of Combination 1

	Asymmetrical			Symmetrical		
Severity Parameter	RDR	SDR	SAR	RDR	SDR	SAR
0	0	1		0	1	
0.01	2.73E-04	1.000011	2.807337	2.78E-04	1.00E+00	1.52E+00
0.02	0.001041	1.000002	1.563456	1.06E-03	1.00E+00	1.49E+00
0.03	0.002263	1.000012	1.601045	0.002305	1.000006	1.590384
0.04	0.00388	1.000018	1.442915	0.003953	1.00001	1.459849
0.05	0.005872	1.00009	1.584002	0.005981	1.000018	1.262206
0.06	0.008148	1.000101	1.254842	0.008313	1.000098	1.70E-05
0.07	0.010756	1.00031	0.99804	1.10E-02	1.00E+00	2.95E-07
0.08	0.01362	1.000709	2.01E-10	1.38E-02	1.00E+00	1.39E+00
0.09	0.016697	1.001297	1.253051	0.017054	1.001271	0.106571
0.1	0.019955	1.002156	1.412378	0.020414	1.002116	1.327395
0.11	0.023518	1.003254	1.12E-12	0.023967	1.0032	1.38E-12
0.12	0.027162	1.004639	2.54E-12	0.02771	1.004558	4.75E-13
0.13	0.030988	1.006319	8.56E-13	0.031584	1.006126	1.62E-13
0.14	0.034919	1.008144	4.49E-13	0.035557	1.008079	1.50E-13
0.15	0.038998	1.01051	6.23E-13	0.03973	1.010204	2.86E-13
0.16	0.043168	1.012882	7.30E-14	0.044011	1.012846	9.96E-14
0.17	0.04742	1.015622	7.29E-14	0.048295	1.015489	5.59E-13
0.18	0.05175	1.01854	2.64E-13	0.052665	1.018604	5.61E-13
0.19	0.056188	1.022079	1.48E-13	0.057162	1.021849	8.14E-13
0.2	0.060692	1.025469	3.90E-13	0.061887	1.025	5.92E-13
0.3	0.128243	1.07345	1.05E-12	0.125943	1.072077	5.06E-13
0.4	0.207568	1.135995	6.23E-13	0.203445	1.133415	6.28E-13

0.5	0.286867	1.216556	2.72E-14	0.280886	1.212135	9.23E-13
0.6	0.361552	1.287393	1.77E-14	0.354229	1.28116	8.46E-13
0.7	0.42965	1.351749	3.48E-18	0.420608	1.34376	8.99E-13
0.8	0.491487	1.430706	3.07E-18	0.480236	1.417843	7.05E-13
0.9	0.546365	1.503119	2.95E-18	0.533152	1.490526	7.05E-15
1	0.594205	1.564987	4.46E-18	0.579359	1.550457	9.76E-15
2	0.844141	1.843351	1.20E-11	0.819488	1.818555	3.49E-15
3	0.931547	1.931516	0.10054	0.893815	1.893786	1.30E-12
4	0.971241	1.971239	0.071569	0.923116	1.923116	1.55E-13
5	1.002209	2.002209	0.059795	0.936644	1.936644	4.06E-13
6	1.022768	2.022768	0.051058	0.946704	1.946704	3.52E-13
7	1.037328	2.037328	4.18E-12	0.953048	1.953048	2.53E-13
8	1.048069	2.048069	1.68E-12	0.957217	1.957217	2.77E-12
9	1.056191	2.056191	0.028975	0.960111	1.960111	5.61E-13
10	1.062523	2.062523	0.030141	0.962185	1.962185	1.88E-13
11	1.067454	2.067454	0.025532	0.963736	1.963736	2.36E-13
12	1.071386	2.071386	0.021914	0.964925	1.964925	6.76E-13
13	1.074571	2.074571	0.01902	0.965852	1.965852	2.96E-12
14	1.077158	2.077158	0.017448	0.97124	1.966589	5.93E-13
15	1.079316	2.079316	0.015796	0.97444	1.967185	1.01E-12
20	1.085342	2.085942	0.010094	0.984971	1.968951	5.48E-12
30	1.090995	2.090995	0.004557	0.993798	1.970218	1.11E-09
40	1.092799	2.092799	0.002751	0.99411	1.970653	3.95E-07
50	1.093637	2.093637	0.001882	0.997961	1.970868	1.61E-04

5. Performance Indices Generated After Simulating The Asymmetrical System ($\beta = 2.80$) and Symmetrical System of Combination 3

	Asymmetrical			Symmetrical		
Severity Parameter	RDR	SDR	SAR	RDR	SDR	SAR
0	0	1		0	1	
0.01	2.71E-04	1.000001	1.484064	2.60E-04	1.000001	1.124583
0.02	0.001041	1	1.58041	9.98E-04	1	1.558803
0.03	0.002262	1.000008	1.57613	0.002164	1.000001	1.595825
0.04	0.003887	1.000005	1.490333	0.003717	1.000011	1.491945
0.05	0.005867	1.000022	1.536588	0.00561	1.000015	1.326989
0.06	0.008162	1.000012	1.205228	0.007822	1.000018	1.244545
0.07	0.01077	1.000011	0.954753	0.010306	1.000021	0.997351
0.08	0.013625	1.000019	0.76637	0.013027	1.000026	8.07E-01
0.09	0.016678	1.000018	0.619288	0.015971	1.000028	0.660154
0.1	0.019985	1.000136	0.511475	0.019156	1.000035	1.36498
0.11	0.023518	1.000054	1.455113	0.022466	1.000037	1.38E+00
0.12	0.02716	1.000052	1.324041	0.025854	1.000037	3.05E-12
0.13	0.030986	1.00011	1.21E-13	0.029469	1.000112	1.48E-11
0.14	0.034917	1.00023	1.05E-12	0.033234	1.000256	1.36E-12
0.15	0.038995	1.00049	4.81E-13	0.037134	1.000518	4.89E-13
0.16	0.043166	1.000819	2.95E-13	0.041153	1.000883	3.98E-13
0.17	0.047419	1.001325	1.16E-13	0.045252	1.001387	9.80E-13
0.18	0.051745	1.002018	8.64E-13	0.049481	1.002158	4.11E-13
0.19	0.056183	1.002734	1.86E-13	0.053716	1.003086	3.55E-13
0.2	0.060687	1.003829	4.52E-13	0.058023	1.004247	4.15E-13
0.3	0.107664	1.027555	2.88E-13	0.106052	1.029195	3.22E-13
0.4	0.165559	1.072037	2.10E-12	0.17394	1.076353	1.81E-12

0.5	0.229844	1.12697	1.53E-14	0.241783	1.133707	2.32E-14
0.6	0.290289	1.171893	6.92E-19	0.3062	1.182475	2.76E-14
0.7	0.345304	1.260312	1.12E-18	0.365146	1.27747	2.64E-14
0.8	0.394622	1.33574	3.13E-19	0.418039	1.357222	3.28E-18
0.9	0.437837	1.397107	1.56E-14	0.464968	1.4226	1.12E-14
1	0.477521	1.447598	9.64E-15	0.507199	1.476699	8.36E-15
2	0.667447	1.666604	7.29E-13	0.724624	1.72364	2.80E-13
3	0.721523	1.716234	2.75E-13	0.792341	1.792306	9.75E-14
4	0.794225	1.730249	1.50E-13	0.818822	1.818821	1.31E-13
5	0.839183	1.734191	4.51E-13	0.832414	1.832414	3.57E-13
6	0.870351	1.735027	3.77E-13	0.859641	1.838312	5.61E-13
7	0.893244	1.734752	3.58E-13	0.887809	1.843965	2.00E-12
8	0.916795	1.734167	1.50E-12	0.904293	1.847075	9.82E-14
9	0.932269	1.731661	5.15E-13	0.911906	1.848856	1.01E-13
10	0.941789	1.728785	5.31E-13	0.92902	1.849439	5.25E-13
11	0.946843	1.727045	1.91E-13	0.941127	1.84953	4.01E-13
12	0.94875	1.727025	1.83E-13	0.949705	1.852207	2.69E-13
13	0.958361	1.724311	6.66E-13	0.951082	1.85282	7.05E-13
14	0.959432	1.723252	1.11E-12	0.953147	1.853168	4.86E-13
15	0.964739	1.722348	1.89E-12	0.960127	1.853786	1.50E-12
20	0.982914	1.719387	4.53E-12	0.976958	1.853445	2.52E-11
30	0.992635	1.717029	8.47E-10	0.990232	1.855716	4.07E-10
40	0.994048	1.716154	1.11E-07	0.993699	1.854644	4.07E-10
50	0.997505	1.716284	8.42E-05	0.995353	1.855063	1.32E-06

ENCLOSURE 2

Ride Comfort Evaluation Data For Modified Bump Input

1. Performance Indices Generated After Simulating All Combinations at Severity Parameter γ of 1

					Asymmetrical			Symmetrical		
Combination	C_s^+	C_s^-	β	α	RDR	SDR	SAR*10	RDR	SDR	SAR*10
1	350	1430	0.24	890	1.265	1.551	8.06E-29	1.242	1.477	7.62E-29
2	2000	1430	1.40	1715	1.130	1.407	7.49E-29	1.139	1.441	7.35E-29
3	4000	1430	2.80	2715	0.991	1.255	7.47E-29	1.086	1.401	7.54E-29
4	350	2000	0.18	1175	1.275	1.567	7.91E-29	1.120	1.463	7.55E-29
5	2000	2000	1	2000	1.123	1.429	7.16E-29	1.123	1.429	7.16E-29
6	4000	2000	2	3000	0.972	1.281	7.21E-29	1.073	1.394	7.55E-29
7	350	4000	0.09	2175	1.320	1.629	7.59E-29	1.112	1.422	7.31E-29
8	2000	4000	0.5	3000	1.174	1.497	7.53E-29	1.073	1.394	7.55E-29
9	4000	4000	1	4000	1.028	1.363	7.56E-29	1.028	1.363	7.56E-29

2. Performance Indices Generated After Simulating All Combinations at Severity Parameter γ of 5

					Asymmetrical			Symmetrical		
Combination	C_s^+	C_s^-	β	α	RDR	SDR	SAR*10	RDR	SDR	SAR*10
1	350	1430	0.24	890	0.997	0.587	1.69E-29	0.999	0.456	1.61E-29
2	2000	1430	1.40	1715	0.999	0.387	1.91E-29	0.999	0.438	2.71E-29
3	4000	1430	2.80	2715	0.999	0.267	3.24E-29	0.995	0.425	3.34E-29
4	350	2000	0.18	1175	0.998	0.633	1.72E-29	0.999	0.449	1.63E-29
5	2000	2000	1	2000	0.998	0.432	1.96E-29	0.998	0.432	1.96E-29
6	4000	2000	2	3000	0.998	0.293	3.31E-29	0.994	0.293	2.41E-29
7	350	4000	0.09	2175	0.998	0.756	1.93E-29	0.998	0.429	3.44E-29
8	2000	4000	0.5	3000	0.998	0.564	2.20E-29	0.994	0.423	2.41E-29
9	4000	4000	1	4000	0.996	0.407	3.57E-29	0.996	0.407	3.57E-29

3. Performance Indices Generated After Simulating All Combinations at Severity Parameter γ of 20

					Asymmetrical			Symmetrical		
Combination	C_s^+	C_s^-	β	α	RDR	SDR	SAR*10	RDR	SDR	SAR*10
1	350	1430	0.24	890	0.999	0.183	3.62E-30	0.999	0.121	3.51E-30
2	2000	1430	1.40	1715	0.999	0.093	3.62E-30	0.999	0.115	3.66E-30
3	4000	1430	2.80	2715	0.999	0.088	3.64E-30	0.999	0.109	4.23E-30
4	350	2000	0.18	1175	0.999	0.205	3.82E-30	0.999	0.118	3.56E-30
5	2000	2000	1	2000	0.999	0.114	3.89E-30	0.999	0.114	3.89E-30
6	4000	2000	2	3000	0.999	0.076	3.82E-30	0.999	0.108	4.41E-30
7	350	4000	0.09	2175	0.999	0.265	4.84E-30	0.999	0.113	3.99E-30
8	2000	4000	0.5	3000	0.999	0.175	4.96E-30	0.999	0.108	4.41E-30
9	4000	4000	1	4000	0.999	0.107	4.92E-30	0.999	0.107	4.92E-30

4. Performance Indices Generated After Simulating The Asymmetrical System ($\beta = 0.24$) and Symmetrical System of Combination 1

	Asymmetrical			Symmetrical		
Severity Parameter	RDR	SDR	SAR	RDR	SDR	SAR
0	0	1	0	0	1	0
0.01	0.031834	1.00581	3.37E-29	0.031697	1.005659	1.89E-29
0.02	0.064948	1.029073	2.60E-29	0.063416	1.028422	1.84E-29
0.03	0.098915	1.054497	2.66E-29	0.096584	1.053178	1.81E-29
0.04	0.13347	1.081693	3.34E-29	0.130636	1.079999	1.84E-29
0.05	0.168716	1.123387	3.39E-29	0.164819	1.120443	1.87E-29
0.06	0.203786	1.143029	2.12E-29	0.198651	1.140296	1.89E-29
0.07	0.238773	1.194738	2.13E-29	0.233303	1.190916	1.90E-29
0.08	0.273898	1.226544	2.15E-29	0.26783	1.221413	1.92E-29
0.09	0.309057	1.242772	2.67E-29	0.302088	1.236752	1.92E-29
0.1	0.34383	1.247166	1.99E-29	0.335995	1.240013	1.92E-29
0.11	0.378063	1.268643	2.00E-29	0.369343	1.261526	1.93E-29
0.12	0.411684	1.329607	1.99E-29	0.402068	1.321293	1.92E-29
0.13	0.444554	1.384206	1.99E-29	0.434125	1.374881	1.92E-29
0.14	0.476673	1.433228	1.98E-29	0.465427	1.422801	1.91E-29
0.15	0.507912	1.478322	1.97E-29	0.495919	1.466509	1.90E-29
0.16	0.538625	1.521089	1.96E-29	0.525544	1.508297	1.89E-29
0.17	0.567594	1.559008	1.95E-29	0.554237	1.545631	1.87E-29
0.18	0.596935	1.592957	1.93E-29	0.582398	1.579127	1.86E-29
0.19	0.624699	1.623146	1.92E-29	0.609692	1.609333	1.85E-29
0.2	0.652497	1.652497	1.90E-29	0.63626	1.63626	1.82E-29
0.3	0.879272	1.818679	1.67E-29	0.85673	1.790931	1.61E-29
0.4	1.039572	1.866121	1.46E-29	1.006942	1.830314	1.40E-29

0.5	1.145538	1.855423	1.36E-29	1.126116	1.811089	1.28E-29
0.6	1.210451	1.809063	1.25E-29	1.207081	1.757496	1.16E-29
0.7	1.252979	1.749361	1.13E-29	1.250531	1.693357	1.04E-29
0.8	1.273823	1.685325	1.01E-29	1.266649	1.620306	9.31E-30
0.9	1.276126	1.617809	9.03E-30	1.263786	1.546766	8.37E-30
1	1.264839	1.55101	8.06E-30	1.241525	1.476815	7.62E-30
2	1.032173	1.087107	4.49E-30	0.985702	0.986634	4.55E-30
3	0.993992	0.846188	2.93E-30	0.996341	0.723327	3.11E-30
4	0.993356	0.700039	2.18E-30	0.995872	0.561281	2.20E-30
5	0.998684	0.587206	1.69E-30	0.999046	0.456023	1.61E-30
6	0.998468	0.514761	1.32E-30	0.998964	0.386522	1.29E-30
7	0.999693	0.459626	1.06E-30	0.999771	0.336611	1.04E-30
8	0.999665	0.40733	8.73E-31	0.999763	0.293426	8.52E-31
9	0.999726	0.369376	7.31E-31	0.999819	0.262128	7.04E-31
10	0.999635	0.342907	6.19E-31	0.999806	0.238096	5.96E-31
11	0.99974	0.315275	6.03E-31	0.99984	0.217943	5.31E-31
12	0.999945	0.293448	4.57E-31	0.999936	0.198846	6.83E-31
13	0.999946	0.270728	5.18E-31	0.999959	0.184636	6.97E-31
14	0.999943	0.251525	5.26E-31	0.999957	0.171128	4.91E-31
15	0.999938	0.236042	4.65E-31	0.999955	0.160186	4.34E-31
20	0.999987	0.182645	3.62E-31	0.99999	0.121275	3.51E-31
30	0.999982	0.126704	1.69E-31	0.999987	0.084396	1.62E-31
40	0.999998	0.093196	9.54E-32	0.999999	0.060866	9.27E-32
50	1	0.077329	6.26E-32	0.999998	0.049153	5.92E-32

5. Performance Indices Generated After Simulating The Asymmetrical System ($\beta = 2.80$) and Symmetrical System of Combination 3

	Asymmetrical			Symmetrical		
Severity Parameter	RDR	SDR	SAR	RDR	SDR	SAR
0	0	1	0	0	1	0
0.01	3.11E-02	1.000023	1.80E-29	2.98E-02	1.00E+00	1.70E-29
0.02	0.060838	1.00491	1.75E-29	5.83E-02	1.01E+00	1.66E-29
0.03	0.089238	1.013489	1.72E-29	0.085443	1.014718	1.62E-29
0.04	0.115965	1.029362	1.68E-29	0.111434	1.03146	1.57E-29
0.05	0.141772	1.057244	1.63E-29	0.139965	1.060815	1.58E-29
0.06	0.166945	1.077299	1.59E-29	0.169814	1.082162	1.59E-29
0.07	0.191047	1.11724	1.56E-29	2.00E-01	1.12E+00	1.60E-29
0.08	0.217177	1.137641	1.56E-29	2.30E-01	1.15E+00	1.61E-29
0.09	0.245359	1.141599	1.55E-29	0.259818	1.151174	1.62E-29
0.1	0.273135	1.138527	1.56E-29	0.289089	1.147982	1.63E-29
0.11	0.301175	1.192431	1.57E-29	0.318616	1.207504	1.62E-29
0.12	0.327681	1.244916	1.57E-29	0.346922	1.262178	1.63E-29
0.13	0.354332	1.29416	1.56E-29	0.375597	1.311172	1.62E-29
0.14	0.380258	1.338569	1.56E-29	0.403437	1.357912	1.61E-29
0.15	0.405723	1.378675	1.55E-29	0.430647	1.400302	1.61E-29
0.16	0.430555	1.414533	1.54E-29	0.456886	1.438415	1.59E-29
0.17	0.455996	1.446598	1.52E-29	0.482125	1.472488	1.59E-29
0.18	0.479924	1.475282	1.51E-29	0.507389	1.50377	1.59E-29
0.19	0.501542	1.501347	1.51E-29	0.531905	1.53145	1.58E-29
0.2	0.524274	1.524274	1.50E-29	0.556608	1.556464	1.56E-29
0.3	0.710192	1.649494	1.34E-29	0.757957	1.697186	1.41E-29
0.4	0.832362	1.664873	1.19E-29	0.898335	1.735547	1.26E-29

0.5	0.909281	1.627791	1.05E-29	0.991103	1.712602	1.13E-29
0.6	0.976943	1.55712	9.63E-30	1.049766	1.663973	1.00E-29
0.7	1.010609	1.48751	9.01E-30	1.081627	1.602289	8.97E-30
0.8	1.019394	1.40938	8.45E-30	1.094257	1.534131	8.45E-30
0.9	1.012089	1.33613	7.94E-30	1.096205	1.470139	7.97E-30
1	0.990884	1.255143	7.47E-30	1.085794	1.40139	7.54E-30
2	0.959579	0.747659	8.50E-30	0.972335	0.935055	4.65E-30
3	0.993734	0.482197	4.66E-30	0.983831	0.671977	3.77E-30
4	0.993042	0.339286	2.88E-30	0.996589	0.520314	2.44E-30
5	0.998745	0.267385	3.24E-30	0.995444	0.425065	3.34E-30
6	0.998701	0.22946	1.40E-30	0.999391	0.364056	2.11E-30
7	0.99973	0.208713	1.91E-30	0.999306	0.305401	1.24E-30
8	0.999662	0.184404	8.65E-31	0.999125	0.268064	1.18E-30
9	0.999819	0.170079	1.03E-30	0.998409	0.253135	1.41E-30
10	0.999777	0.156424	9.36E-31	0.999854	0.22046	9.36E-31
11	0.999799	0.145519	5.48E-31	0.99987	0.198981	6.89E-31
12	0.999816	0.136452	8.02E-31	0.999939	0.188529	6.23E-31
13	0.999938	0.12684	5.11E-31	0.999838	0.166401	5.71E-31
14	0.999936	0.118627	4.86E-31	0.999772	0.157097	5.37E-31
15	0.999933	0.111983	4.30E-31	0.999687	0.152278	4.82E-31
20	0.999988	0.08823	3.64E-31	0.999971	0.109163	4.23E-31
30	0.999986	0.060728	1.70E-31	0.999979	0.073413	2.02E-31
40	0.999998	0.04531	9.63E-32	0.999996	0.054757	1.18E-31
50	0.999998	0.036455	6.15E-32	0.999996	0.043997	7.59E-32

ENCLOSURE 3

Ride Comfort Evaluation Data For Sinusoidal Input

	Root-Mean-Square Acceleration of Sprung Mass (m/s2)								
Combination / Velocity (km/hr)	1	2	3	4	5	6	7	8	9
0	0	0	0	0	0	0	0	0	0
10	0.508	0.503	0.499	0.505	0.504	0.500	0.504	0.498	0.486
20	0.706	0.734	0.734	0.729	0.729	0.743	0.766	0.746	0.810
30	0.540	0.559	0.622	0.556	0.610	0.615	0.636	0.641	0.658
40	0.639	0.605	0.662	0.652	0.647	0.675	0.667	0.687	0.772
50	0.740	0.809	0.828	0.755	0.797	0.841	0.750	0.842	0.886
60	0.974	0.971	1.097	0.974	0.971	1.121	0.979	1.116	1.280
70	1.606	1.497	1.698	1.575	1.492	1.667	1.589	1.668	1.551
80	3.601	2.590	1.954	2.914	2.400	1.843	2.227	1.848	1.526
90	1.786	1.950	1.720	1.874	1.885	1.681	1.793	1.683	1.592
100	1.082	1.209	1.276	1.138	1.235	1.299	1.229	1.301	1.357
110	0.664	0.783	0.915	0.697	0.870	0.998	0.780	0.998	1.112
120	0.481	0.591	0.722	0.509	0.631	0.765	0.622	0.766	0.891

REFERENCES

[1] Rajamani, R. 2012. **Vehicle Dynamics and Control (Second Edition).** Springer: Mechanical Engineering Series.

[2] Silveira, M., Pontes Jr., B.R., and Balthazar, J.M. 2014. "Use of nonlinear symmetrical shock absorber to improve comfort on passenger vehicles". **Journal of Sound and Vibration** 333, pp. 2114-2129.

[3] Sun, L. 2001. "Optimum design of "road friendly" vehicle suspension systems subjected to rough pavement surfaces". **Applied Mathematical Modelling** 26, pp. 635-652.

[4] Rao, S.S. 2010. **Mechanical Vibrations (5th Edition).** N.J.: Prentice Hall.

[5] Kiencke, U. 2005. **Automotive Control Systems For Engine, Driveline, and Vehicle.** Springer Berlin.

[6] Wallaschek, J. 1990. "Dynamics of Non-Linear Automobile Shock-Absorbers". **International Journal of Non-Linear Mechanics**, Vol. 25, No 2/3, pp. 299-308.

[7] Experimental Data and Data acquired from Laboratory of Vibration and

[8] Ulsoy, A.G. 2012. **Automotive Control Systems.** Cambridge University Press.

[9] Close, C.M. 2001. **Modelling and Analysis of Dynamic Systems (Third Edition).** John Wiley & Sons, Inc.

[10] Anirban,C.M. 2013. “Ride comfort and vehicle handling of quarter car model using SIMULINk and Bond Graph”. **Proceedings of the 1st International and 16th National Conference on Machines and Mechanisms** (iNaCoMM2013), IIT Roorke, India.

[11] Ahmed,A.K.W., and Rakheja, S. 1992. “An equivalent linearization technique for the frequency response analysis of asymmetric dampers”. **Journal of Sound and Vibration** 153, 3:537-542.

[12] Ahmed,A.K.W., and Rakheja, S. 1994. “An algorithm for simulation of nonlinear mechanical system using energy and force similarity of its elements”. **Finite Elements in Analysis and Design** 18, pp. 141-154.

[13] International Standard Organization. 1997. **ISO 2631-1 Mechanical vibration and shock – Evaluation of human exposure to whole-body vibration Part 1: General requirements.**

[14] Rajalingham, C. and Rakheja, S. 2003. “Influence of suspension damper asymmetry on vehicle vibration response to ground excitation”. **Journal of Sound and Vibration** 266, pp. 1117-1129.

BIOGRAPHY

Listy Fazria Setiawan was born in Pekanbaru on 22nd January 1993. Her parents are originally from Bandung, but her father's job – a petroleum engineer - requires a lot of moving. In 2003 the family moved to Kuala Lumpur, Malaysia and they ended up residing there. She has two younger sisters: one currently a university student and the other one a middle schooler. After taking the GCE A Levels at Methodist College Kuala Lumpur (MCKL) in 2010, she then made a decision to pursue higher education in Indonesia and attended Institut Teknologi Sepuluh Nopember, where she studied Mechanical Engineering and is registered to NRP 2111100180.

During the duration of study, Listy was an active member of ITS Foreign Language Society (IFLS), previously registered as part of the English Department. She was quite enthusiastic in scientific writing and was a finalist in Pekan Ilmiah Mahasiswa Nasional (PIMNAS) 26 in 2014. In 2014 she was also chosen as a participant of the JENESYS program in which she spent a week in Japan and met new people both Japanese and ASEAN-born. For her final project, Listy took a subject of asymmetrical damping and thus became a member of Laboratory of Vibrations and Dynamical Systems.

Any information, questions or suggestions readers might have for Author, please contact Author through email listyfazria@gmail.com.